Extramacrochaetae regulates Notch signaling in the *Drosophila* eye through non-apoptotic caspase activity

Sudershana Nair[1,4]
Nicholas E. Baker[1,2,3,5]

1. Department of Genetics
Albert Einstein College of Medicine
1300 Morris Park Avenue
Bronx
NY 10461

2. Department of Developmental and Molecular Biology
Albert Einstein College of Medicine
1300 Morris Park Avenue
Bronx
NY 10461

3. Department of Ophthalmology and Visual Sciences
Albert Einstein College of Medicine
1300 Morris Park Avenue
Bronx
NY 10461

4. Present address: Department of Neuroscience and Physiology
NYU School of Medicine
435 East 30th St
New York, NY

5. Author for correspondence: Nicholas.baker@einsteinmed.edu

Abstract

Many cell fate decisions are determined transcriptionally. Accordingly, some fate specification is prevented by Inhibitor of DNA binding (Id) proteins that interfere with certain master regulatory transcription factors. We report that the *Drosophila* Id protein Extra macrochaetae (Emc) also affects developmental decisions by regulating caspase activity. Emc, which prevents proneural bHLH transcription factors from specifying neural cell fate, also prevents homodimerization of another bHLH protein, Daughterless (Da), and thereby maintains expression of the *Death-Associated Inhibitor of Apoptosis* (*diap1*) gene. Multiple effects of *emc* mutations, on cell growth and on eye development, were all caused by reduced Diap1 levels and corresponding activation of caspases. These effects included growth of unspecified imaginal disc cells, acceleration of the morphogenetic furrow, failure of R7 photoreceptor cell specification, and delayed differentiation of non-neuronal cone cells. Within *emc* mutant eye clones, morphogenetic furrow speed was increased by elevated Notch signaling, while decreased Notch signaling inhibited R7 specification and cone cell differentiation. This was all due to caspase-dependent increase in levels of Delta protein, a transmembrane ligand that both trans-activates and cis-inhibits Notch. Thus, *emc* mutations reveal the importance of restraining caspase activity, even in non-apoptotic cells, to prevent abnormal development.

52 **Introduction**

53

54 Certain families of master regulatory transcription factor control major developmental
55 decisions in metazoa. This includes the bHLH proteins encoded by proneural genes, which were
56 discovered in *Drosophila* and control neural fate specification and differentiation from sponges
57 to humans(Weinberger et al., 2017; Baker & Brown, 2018; Dennis, Han, & Schuurmans, 2019;
58 Johnson, 2020). One of the ways proneural gene activities are regulated, thereby modulating the
59 location and timing of neurogenesis, is through Inhibitor of DNA binding proteins (Id proteins),
60 which are HLH proteins lacking basic DNA-binding sequences. Using their HLH domains, Id
61 proteins form inactive heterodimers with proneural bHLH proteins, preventing DNA binding and
62 transcriptional regulation of target genes by the resulting heterodimer (Benezra, Davis,
63 Lockshon, Turner, & Weintraub, 1990; Ellis, Spann, & Posakony, 1990; Garrell & Modolell,
64 1990; Cabrera, Alonso, & Huikeshoven, 1994; Ellis, 1994; Norton, 2000). Accordingly,
65 mutations in Id protein genes, of which there are 4 in mammals and one in *Drosophila*, permit
66 enhanced proneural bHLH function, deregulating neurogenesis at many developmental stages
67 and in many tissues. Mammalian Id gene expression is particularly associated with proliferative
68 and stem cell states, and is frequently affected in cancer(Ling, Kang, & Sun, 2014; Wang &
69 Baker, 2015a; Roschger & Cabrele, 2017; Oproescu, Han, & Schuurmans, 2021).

70 An outstanding question has been whether heterodimerization with proneural bHLH
71 proteins represents the only mechanism of Id protein function. This question arises because not
72 all phenotypes of Id gene mutations obviously represent gain of proneural gene function.
73 Interpretation is complicated in mammals by the number of proneural bHLH genes and of Id
74 protein genes, both functionally redundant so that single mutant phenotypes reflect only subsets
75 of protein function(Ling et al., 2014; Wang & Baker, 2015a). In *Drosophila*, it is clear that
76 mutating the sole Id protein gene *extra macrochaetae* (*emc*) affects some tissues where no
77 proneural gene is known to function. The first example noted was the requirement for *emc* for
78 normal growth of imaginal discs(Garcia-Alonso & Garcia-Bellido, 1988). Imaginal discs are
79 larval progenitors of adult tissues and remain proliferative and undifferentiated until late in the
80 final larval instar; no proneural gene is active in these proliferating cells. A second example is
81 that *emc* is required for ovarian follicle cell development (Adam & Montell, 2004), which does

82 not depend on proneural bHLH genes. Further examples are noted in *Drosophila* eye
83 development. The *emc* gene is required to restrain the rate at which the morphogenetic furrow, a
84 wave of fate specification that traverses across the eye imaginal disc as retinal patterning and
85 differentiation begin(Brown, Sattler, Paddock, & Carroll, 1995). *emc* is also required for the
86 specification of the R7 photoreceptor cells and the non-neuronal cone cells, neither of which
87 depends on any known proneural bHLH gene (Bhattacharya & Baker, 2009). Most recently, *emc*
88 was also found to be required for left-right asymmetry of the *Drosophila* gut(Ishibashi et al.,
89 2019). Thus, *Drosophila* provides opportunities to investigate how at least one Id protein
90 functions independently of proneural bHLH proteins, and potentially reveal new mechanisms of
91 developmental regulation.

92 Insights into how Emc acts independently of proneural genes have progressively emerged
93 from several studies. The first concerned the proper proliferation of imaginal disc cells(Garcia-
94 Alonso & Garcia-Bellido, 1988). Independence of imaginal disc growth from proneural bHLH
95 genes is confirmed by the lack of requirement for *da*, the only E protein in
96 *Drosophila*(Bhattacharya & Baker, 2011; Andrade-Zapata & Baonza, 2014). E proteins are
97 ubiquitously-expressed bHLH proteins that are heterodimer partners for proneural bHLH
98 proteins. In Drosophila, proneural bHLH proteins cannot function without Da, so normal growth
99 of *da* mutant cells implies independence from all Da heterodimer partners. Remarkably, it is
100 actually ectopic Da activity that causes poor growth in *emc* mutant cells, normal growth being
101 restored in *emc da* doubly mutant cells (Bhattacharya & Baker, 2011). Without *emc*, Da levels
102 are elevated and by themselves activate transcription of *expanded* (*ex*), a component of the
103 Salvador-Hippo-Warts (SHW) tumor suppressor pathway. This increased SHW pathway activity
104 is what inhibits growth of imaginal disc cells(Wang & Baker, 2015b). Thus, one role of *emc* is
105 to restrain Da(Reddy, Bhattacharya, & Baker; Bhattacharya & Baker, 2011; Wang & Baker,
106 2015a; Li & Baker, 2018).

107 In the course of these studies, we noticed that *ex* mutations affected the number of
108 sensory organ precursor (SOP) cells in the thorax(Wang & Baker, 2015b). We showed that this
109 was due to activity of Yorkie (Yki), the transcription factor target of SHW signals, in the *ex*
110 mutant cells. This in turn increased transcription of a direct Yki target gene, *Death-Associated*
111 *Inhibitor of Apoptosis 1* (*diap1*)(Wang & Baker, 2019). Diap1 is a ubiquitin ligase that prevents

112 accumulation of a processed form of Dronc, an apical caspase in *Drosophila*(Muro, Hay, &
113 Clem, 2002; Wilson et al., 2002; Yan, Wu, Chai, Li, & Shi, 2004; Li, Wang, & Shi, 2011).
114 Caspases are proteases that are well known for driving apoptosis by cleaving cellular substrates.
115 They are expressed as inactive zymogens that are then activated by signals (initiator caspases) or
116 by cleavage by caspases (effector caspases) in a feed-forward process that is expected to kill
117 cells rapidly once a threshold of caspase activity has been crossed(Fuchs & Steller, 2011). Many
118 studies show that caspases can also mediate non-apoptotic processes, although what
119 differentiates apoptotic from non-apoptotic outcomes is uncertain, as the same caspase cascade
120 of initiator and effector caspases seems to be involved (Yamaguchi & Miura, 2015; Aram,
121 Yacobi-Sharon, & Arama, 2017; Nakajima & Kuranaga, 2017; Baena-Lopez, Arthurton, Xu, &
122 Galasso, 2018; Colon-Plaza & Su, 2022). Non-apoptotic caspase activities are of particular
123 interest because of their contributions to multiple diseases(Su, 2020). In *ex* mutants, the
124 increased *diap1* transcription does not affect cell death much, but causes an increase in *wg*
125 signaling activity in the thorax(Wang & Baker, 2019). Wg signaling promotes SOP cell
126 determination in the thorax, and it has been shown previously that Wg signaling is antagonized
127 by caspases, through a mechanism that is non-apoptotic but whose direct target is not yet
128 certain(Baker, 1988; Kanuka et al., 2005; Wang & Baker, 2019).

129 Since *emc* mutations elevate *ex* expression(Wang & Baker, 2015b), we wondered
130 whether *emc* also changes Diap1 levels and affects caspase activities. Increased *ex* expression in
131 *emc* mutants would be expected to reduce transcription of the *diap1* gene and potentially increase
132 caspase activity, the opposite of what occurs in *ex* mutants. This predicts that caspases could
133 contribute to aspects of the *emc* mutant phenotype, especially those that do not depend on
134 proneural bHLH genes. Remarkably, we found that caspase activity was responsible for all the
135 aspects of the *emc* phenotype that we tested. This included reduced growth of imaginal disc
136 cells, accelerated morphogenetic furrow progression, and loss of R7 and cone cells fates in the
137 eye. The effects on eye development all reflected caspase-dependent expression of the Notch
138 ligand Delta, which is known to contribute to morphogenetic furrow progression, and R7 and
139 cone cell fate specification. Thus, caspase-dependent non-apoptotic signaling underlies multiple
140 roles of *emc* that are independent of proneural bHLH proteins.

141

142 **Materials and Methods**

143

144 **Drosophila Strains**

145

146 The following stocks were employed in this study and were maintained at 25°C unless otherwise
147 stated - *hsflp;;emc^{AP6} FRT80/TM6B, hsflp;;dronc^{i29}FRT80/TM6B, hsflp;;dronc^{i29}emc^{AP6},*
148 *hsflp;;Df(3L)H99/TM3, hsflp;;Df(3L)H99 emc^{AP6}/TM3, Ubi-GFP M(3)67C FRT80, FRT42*
149 *M(2)56F Ubi-GFP, FRT82 M(3)95A Ubi-GFP, hsflp;; Ubi-GFPFRT80, hsflp*; *Su(H)$^{\Delta 47}$FRT40*,
150 *pie^{eB3} FRT40* (Baker et al., 1992), *psn[v1]FRT80/TM6B, Fz3-RFP*;D/TM6B (kind gift from Yu
151 Kimata, University of Cambridge). We obtained genomic Ci construct from Kalderon lab and
152 used BestGene Inc. to target the transgene on the third chromosome and then recombined these
153 flies to generate *hsflp;;ci+M(3)67Calz FRT80/TM6B;ci94/y+spa.*

154

155 **Mosaic Analysis**

156 Mosaic clones were obtained using FLP/FRT mediated mitotic recombination (Golic, 1991; Xu
157 & Rubin, 1993). For non-Minute genotypes, larvae were subjected to heat shock for 30 minutes
158 at 37°C, 60 ± 12 hours after egg laying. For Minute genotypes, heat shock was performed 84 ±
159 12 hours after egg laying for 50 minutes. Larvae were dissected 72 hours after heat shock. All
160 flies were maintained at 25°C unless otherwise stated.

161 **Immunohistochemistry and histology**

162 Unless otherwise noted, preparation of eye and wing imaginal discs for immunostaining and
163 confocal imaging were performed as described previously (Baker, Li, Quiquand, Ruggiero, &
164 Wang, 2014). Antibodies from Developmental Studies Hybridoma Bank (DSHB): anti-Ptc
165 (mouse, 1:40), anti-Elav (mouse, 1:100), anti-Elav (rat, 1:50, anti-Cut (mouse, 1:50), anti-Delta
166 C594.9B (mouse, 1:2000), anti-βGal (mouse, 1:100), mouse anti-βGal (1:100, DSHB 40-1a) and
167 anti-Ci (rat, 1:10). Other antibodies: anti-phospho-Smad1/5 (rabbit, 1:100, Cell Signaling), anti-
168 DIAP1 (mouse, 1:50) (gift from Hyun Don Ryoo, NYU), anti-Dcp1 (rabbit, 1:100, Cell
169 Signaling), anti-Sens (guinea pig, a gift from Hugo Bellen used at 1:50), anti-Da (mouse, 1:200),
170 rabbit anti-Emc (1:40), anti-GFP (rat, 1:50 from Nacalai Tesque # GF090R), rabbit anti-GFP

171 (1:500), rabbit anti-ß-Galactosidase (1:100, Cappel), E(spl)bHLH (1:50,mAb323) and guinea pig
172 anti-runt (1:500). Secondary antibodies conjugated with Cy2, Cy3 and Cy5 dyes (1:200) were
173 from Jackson ImmunoResearch Laboratories and Alexa 555 (1:500). Multi-labelling images
174 were sequentially scanned with Leica SP8 confocal microscopes and were projected and
175 processed with ImageJ. All images were assembled into figure format using Adobe Illustrator
176 2020.
177
178 **Terminal deoxynucleotidyl transferase dUTP nick end labeling (TUNEL) assay**
179
180 For labeling dead cells with TUNEL assay, ApopTag® Red In Situ Apoptosis Detection Kit (Cat
181 #S7165) was used according to manufacturer's instruction. Briefly, dissected eye discs were
182 fixed for 20 minutes at room temperature followed by three washes with 1X PBS. Then the
183 samples were incubated in equilibration buffer for 1 minute followed by incubation in reaction
184 buffer (TdT enzyme; ratio 7:3) at 37 °C for 1 hour. TdT reaction mix was replaced with stop
185 buffer (diluted 1:34 in dH2O) and incubated for 10 min at room temperature. Samples were
186 washed three times with 1X PBS, 5 min per wash; and incubated with anti-digoxigenin antibody
187 solution (diluted 31:34 in blocking solution) for 30 min at room temperature. The samples were
188 then washed three times in 1X PBS, 5 min per wash. For the subsequent antibody staining, the
189 samples were blocked in PBST (1X PBS + 0.5% Triton-X) for 30 min, and incubated with
190 primary antibodies in PBST overnight at 4 °C. The samples were next washed with PBST and
191 incubated for 2 h with secondary antibodies in PBST, and then again washed with PBST,
192 followed by PBS wash and samples were mounted in mounting media.
193
194 **Statistical analysis**
195 Statistical analysis of clone size data reported in Figur 1N is described in the figure legend.
196
197 **Prediction of caspase cleavage sites**
198
199 Caspase cleavage sites were predicted for Delta using Cascleave 2.0(Wang et al., 2014).
200 Cascleave 2.0 was set to a medium stringency threshold for prediction of cleavage sites.
201

202

203 **Results**

204

205 **Caspase activity causes growth defects in *emc* mutants**

206

207 To determine the contribution of caspases to growth inhibition in *emc* mutant cells, we
208 used the FLP/FRT system (Xu & Rubin, 1993) to generate clones of *emc* mutant cells that were
209 unable to activate caspases normally. We achieved this by homozygously deleting the linked
210 *reaper* (*rpr*), *head involution defective* (*hid*) and *grim* genes using *Df(3L)H99*. Rpr, Hid and
211 Grim proteins promote Diap1 degradation in response to apoptotic stimuli and allow activation
212 of initiator caspases such as *dronc* to start apoptosis(Yoo et al., 2002). By removing all three
213 pro-apoptotic proteins, *Df(3L)H99* affects both apoptotic and non-apoptotic caspase functions
214 in *Drosophila* (White et al., 1994; Tapadia & Gautam, 2011). Thus, clones of *emc Df(3L)H99*
215 mutant cells should be defective for caspase activation. In addition, we also made clones of *emc*
216 mutant cells further mutated for *dronc*, which encodes the main initiator caspase in *Drosophila*
217 that is necessary for most developmental apoptosis (C. J. Hawkins et al., 2000; Meier, Silke,
218 Leevers, & Evan, 2000; Quinn et al., 2000). Dronc contributes to non-apoptotic caspase
219 functions as well, so *emc dronc* mutant cells should also show reduced non-apoptotic and well as
220 apoptotic caspase functions.

221 In comparison to neutral clones, which grew equivalently to their twin-spot controls, *emc*
222 mutant clones showed greatly reduced growth in eye or wing imaginal discs, as described
223 previously (Figures 1A-D) (Garcia-Alonso & Garcia-Bellido, 1988; Bhattacharya & Baker,
224 2011; Andrade-Zapata & Baonza, 2014). By contrast, *emc* mutant clones that were also mutant
225 for *dronc*, or *emc Df(3L)H99* clones that lacked the *rpr*, *grim* and *hid* genes, grew more like their
226 twin spot controls in both eye and wing (Figures 1E-H). Deletion of the *rpr*, *hid* and *grim* genes
227 restored growth indistinguishable from the wild type to *emc* clones, although mutation of *dronc*
228 rescued less completely (see Figure 1N for quantification). Neither homozygosity for *dronc*, nor
229 deletion of *rpr*, *grim* and *hid*, affected growth of otherwise wild type imaginal disc clones
230 (Figure 1I-L).

231 Previous studies of *emc* phenotypes have often used Minute genetic backgrounds (ie
232 heterozygosity for mutations in *Rp* genes) to retard growth and enhance the size of the *emc*

233 mutant clones(Bhattacharya & Baker, 2009). When *emc Df(3L)H99* clones were induced in the
234 *M(3)67C* background, the clones took over almost the entire disc, leaving only a few *M(3)67C*
235 heterozygous cells remaining (Figure 1M).
236 These results indicate that the growth disadvantage of *emc* mutant imaginal disc clones is
237 mostly attributable to cell death genes. Preventing caspase activation, either by mutating the
238 main initiator caspase, or by preventing Diap1 turnover, partially or completed restored normal
239 growth. Our data did not support a previous suggestion that *dronc* was required for normal wing
240 disc growth(Verghese, Bedi, & Kango-Singh, 2012).
241
242 **Emc regulates furrow progression through non-apoptotic caspase activity**
243
244 *Emc* mutations have multiple effects on the eye imaginal disc, although only a few
245 aspects of retinal differentiation depend on proneural bHLH genes. The proneural gene *atonal* is
246 required, along with *da*, for the specification of R8 photoreceptor precursors in the
247 morphogenetic furrow that found each ommatidial cluster in the larval eye disc(Jarman, Grell,
248 Ackerman, Jan, & Jan, 1994; Brown et al., 1996). Later, during pupal development, proneural
249 genes of the Achaete-Scute gene Complex (AS-C), along with *da*, are required for the
250 specification of the interommatidial bristles(Cadigan, Jou, & Nusse, 2002). All the other cell
251 types develop independently of proneural bHLH genes, and most of them develop independently
252 of *da* (Jimenez & Campos-Ortega, 1987; Brown et al., 1996).
253 In *emc* mutant clones, retinal differentiation begins precociously, associated with more
254 rapid transit of the morphogenetic furrow across the disc (Figure 2A, B)(Brown et al., 1995;
255 Bhattacharya & Baker, 2011, 2012). By contrast, we found that 75% of the time, the
256 morphogenetic furrow progressed normally through *emc dronc* double mutant clones (Figure
257 2C). Eye discs containing *emc Df(3L)H99* double mutant clones always appeared completely
258 normal (Figure 2D). Both *dronc* and *Df(3L)H99* mutant clones also showed normal furrow
259 progression in the absence of *emc* mutations (Figure 2 Figure Supplement 1A,B).
260 Not only the position of the morphogenetic furrow, but also the overall pattern of retinal
261 differentiation revealed by labeling for Senseless, which is specific for R8 photoreceptor cells,
262 and Elav, which labels all neuronal photoreceptor cells, appeared so normal in these genotypes
263 that we deemed it necessary to confirm that the supposedly *emc dronc* mutant and *emc*

264 *Df(3L)H99* mutant clones were indeed mutated for *emc*. This was confirmed by lack of staining
265 by an antibody against Emc protein, similar to plain *emc* mutant clones that did affect the
266 morphogenetic furrow (Figure 2 Figure supplement 1C-E). We also found that *emc dronc* and
267 *emc Df(3L)H99* clones upregulated Da protein expression to a comparable degree to plain *emc*
268 mutant clones (Figure 2 Figure Supplement 1C-E)(Bhattacharya & Baker, 2011). This further
269 confirmed the absence of *emc* function from *emc dronc* mutant and *emc Df(3L)H99* genotypes,
270 and also showed that cell death pathways were not required for the regulation of Da protein
271 levels by *emc*.
272 We have previously shown that *diap1* transcription is reduced in *emc* mutant clones, and
273 in Da-overexpressing cells, due to Yki inhibition downstream of *ex* (Wang & Baker, 2015b). In
274 eye imaginal discs, Diap1 protein was normally present uniformly (Figure 3A). Diap1 protein
275 levels were cell-autonomously reduced in *emc* mutant clones (Figure 3B). A comparable
276 reduction was also seen in *emc Df(3L)H99* clones, (Figure 3C). Because *emc Df(3L)H99* clones
277 developed normally, this suggested Diap1 protein levels were upstream of the cell death pathway
278 in affecting morphogenetic furrow speed, and that *rpr*, *grim*, and *hid* activities were required
279 downstream of *diap1*. To test the role of Diap1 directly, *diap1* was over-expressed in the
280 posterior eye by transcription under GMR-Gal4 control. This rescued morphogenetic furrow
281 speed to normal in *emc* clones (Figure 3D). We also saw restoration of morphogenetic furrow
282 speed in *emc* clones that expressed Baculovirus P35 under GMR-Gal4 control (Figure 3E).
283 Baculovirus P35 encodes a caspase pseudo-substrate that inhibits all *Drosophila* caspases except
284 Dronc(Hay, Wolff, & Rubin, 1994; Xue & Horvitz, 1995; C.J. Hawkins et al., 2000; Meier et al.,
285 2000). The *emc* clones expressing p35 also lacked cell death (Supplemental Figure 2D). The
286 restoration of morphogenetic furrow speed by Diap1, a *dronc* antagonist, as well as by the
287 caspase inhibitor P35, suggest that the effect of morphogenetic furrow acceleration in *emc*
288 mutant clones is due to the caspase cascade.
289 To test whether reduced Diap1 expression promoted apoptosis and thereby accelerated
290 the morphogenetic furrow, we assessed apoptosis levels by terminal deoxynucleotidyl transferase
291 dUTP nick end labeling (TUNEL) of eye discs containing mutant clones. We found almost no
292 cell death posterior to the furrow in *emc* clones (Supplemental Figure 2B), and cell death in *emc*
293 clones anterior to the furrow was comparable to controls and less than that of cells surrounding
294 the clones (Supplemental Figure 2A). Some cell death is expected outside *emc* or control clones,

295 as these cells have the *M* background that is itself associated with an increase in
296 apoptosis(Coelho et al., 2005; Li & Baker, 2007; Kale, Li, Lee, & Baker, 2015). To test whether
297 apoptosis in the eye disc would be sufficient to promote morphogenetic furrow progression, we
298 generated mosaic clones for a *pineapple eye (pie)* mutation. These *pie* mutant cells have an
299 elevated rate of apoptosis in imaginal discs, but not sufficient to prevent *pie* homozygous clones
300 surviving late into larval and even adult life (Shi, Stampas, Zapata, & Baker, 2003). The rate of
301 morphogenetic furrow progression was unaffected in eye discs containing *pie* clones
302 (Supplemental Figure 2C). Because no excess cell death was detected in *emc* clones, and cell
303 death was insufficient to accelerate the morphogenetic furrow in otherwise wild type eye discs,
304 *emc* clones might be affected by a non-apoptotic caspase activity.
305
306 **Wingless and Dpp signaling are unaffected by *emc***
307 To understand how caspases could affect the speed of the morphogenetic furrow, we
308 analyzed pathways known to contribute. Hedgehog (Hh) and Decapentaplegic (Dpp) signaling
309 drive this differentiation wave, along with a contribution from Notch signaling (U. Heberlein, T.
310 Wolff, & G. M. Rubin, 1993; Ma, Zhou, Beachy, & Moses, 1993; Borod & Heberlein, 1998;
311 Baonza & Freeman, 2001b; Fu & Baker, 2003). A negative regulator of morphogenetic furrow
312 progression is Wingless (Wg), which is expressed at the dorsal and ventral eye disc margins
313 (Maurel-Zaffran & Treisman, 2000; Lee & Treisman, 2002).
314 Because we found that *ex* mutations affected thoracic bristle patterning through a
315 caspase-dependent non-apoptotic effect on Wg signaling (Wang & Baker, 2019), we looked first
316 to see whether *emc* mutations reduced Wg signaling in the eye. We used Frizzled-3 RFP (Fz3-
317 RFP) as a reporter (Sato, Kojima, Ui-Tei, Miyata, & Saigo, 1999). In control eye discs, the Fz3-
318 RFP recapitulates the pattern of endogenous Wg signaling activity at the wing margins (Figure 4
319 figure supplement 1) (Treisman & Rubin, 1995). Frizzled-3 RFP expression was not changed in
320 *emc* clones (Figure 4A). We then used a mutation in *naked cuticle* (*nkd*), encoding a negative
321 feedback regulator of Wg signaling, to modulate Wg signaling(Zeng et al., 2000; Chang, Chang,
322 Barolo, & Cadigan, 2008). If the morphogenetic furrow was accelerated in *emc* mutant clones
323 due to reduced Wg signaling, more normal development should occur in *emc nkd* clones. The
324 morphogenetic furrow was still accelerated in *emc nkd* clones, however (Figure 4B). These
325 results provided no evidence that Wg signaling was the relevant *emc* target in the eye.

326 We also examined Dpp signaling, since ectopic Dpp signaling is sufficient to accelerate
327 the morphogenetic furrow(Pignoni & Zipursky, 1997). The pattern of pMad, a readout of Dpp
328 signaling, was identical in *emc* mutant and control clones spanning the morphogenetic furrow
329 (Figure 4C, D). Thus, Dpp signaling did not seem altered by *emc* mutants either.
330
331 **Hedgehog pathway**
332 Hedgehog signaling is a key mover of the morphogenetic furrow(U. Heberlein, T. Wolff,
333 & G.M. Rubin, 1993; Ma et al., 1993; Treisman, 2013). Elevated Hh signaling is sufficient to
334 accelerate the morphogenetic furrow(Heberlein, Singh, Luk, & Donohoe, 1995; Ma & Moses,
335 1995). Notably, it has been suggested previously that *emc* mutations affect the morphogenetic
336 furrow by activating Hedgehog signaling, because *emc* mutant cells accumulate Ci protein
337 (Spratford & Kumar, 2013). Full-length Ci protein (Ci155) is targeted to the proteosome by
338 Cul1 for processing into a transcriptional repressor protein Ci75(Aza-Blanc, Ramirez-Weber,
339 Laget, Schwartz, & Kornberg, 1997). By inhibiting this processing, Hh prevents repression of
340 target genes by Ci75 and promotes transcriptional activation downstream of Ci155.
341 Accordingly, Ci155 accumulation is a feature of cells receiving Hh signals(Motzny & Holmgren,
342 1995).
343 We confirmed that *emc* mutant cells contain higher levels of Ci155, as reported
344 previously (Figure 5A)(Spratford & Kumar, 2013). Ci155 was elevated in *emc dronc* clones
345 (Figure 5B) but reduced to wild-type levels in *emc Df(3L)H99* clones (Figure 5C, Figure 5 figure
346 supplement 1). Thus, Ci155 levels did not correlate perfectly with behavior of the morphogenetic
347 furrow.
348 We noticed that Ci155 levels were elevated in *emc* mutant clones in the posterior,
349 differentiating eye disc, as well as in and ahead of the morphogenetic furrow (Figure 5A). This
350 is significant, because Ci155 is not affected by Hh-dependent Cul1 processing posterior to the
351 morphogenetic furrow (Ou, Lin, Chen, & Chien, 2002; Baker, Bhattacharya, & Firth, 2009).
352 Ci155 accumulation posterior to the furrow suggests a Hh-independent mechanism.
353 To test whether Ci155 accumulation in *emc* clones indicates elevated Hh target signaling,
354 we looked at the transmembrane receptor Patched (Ptc) which is a transcriptional target of Hh
355 signaling, acting in a negative feedback loop(Hepker, Wang, Motzny, Holmgren, & Orenic,
356 1997). We saw no changes in Ptc protein levels in either *emc* or *emc Df(3L)H99* clones

357 compared to controls, questioning the notion that Hh signaling was altered by *emc* (Figure 5
358 figure supplement 2).
359 To test definitively whether Ci155 is responsible for accelerating the furrow in *emc*
360 clones, we generated *emc ci* double mutant clones. To achieve this, a genomic transgene that
361 rescues ci^{94} flies to adulthood (Little, Garcia-Garcia, Sul, & Kalderon, 2020), was introduced
362 into chromosome arm 3L where it is linked to the wild type *emc* locus, so that mitotic
363 recombination in the ci^{94} null background leads to *emc ci* double mutant clones. For unknown
364 reasons, *emc ci* double mutant clones were small and difficult to obtain, even in the Minute
365 background. In all the *emc ci* double mutant clones we found that spanned the morphogenetic
366 furrow; eye differentiation was still accelerated (Figure 5D). These data might not exclude a
367 quantitative contribution of Ci to more rapid morphogenetic furrow progression in the absence of
368 *emc* but are sufficient to show that *emc* regulates the speed of the morphogenetic furrow through
369 at least one other caspase target.
370
371 **Delta expression is a target of caspases**
372
373 The remaining signaling pathway that contributes to morphogenetic furrow movement is
374 Notch. Specifically, only cells where Notch signaling is active are competent to initiate retinal
375 differentiation in response to Dpp (Baonza & Freeman, 2001a; Fu & Baker, 2003). Accordingly,
376 ectopic expression of Delta, the transmembrane ligand for Notch, is sufficient to accelerate
377 retinal differentiation anterior to the morphogenetic furrow by expanding the effective range of
378 Dpp signaling (Baonza & Freeman, 2001a; Li & Baker, 2001).
379 To test whether *emc* restrains Notch, we examined the bHLH proteins of the E(spl)-C,
380 widely characterized targets of the Notch pathway (Bray, 2006). We used mAb323 to detect up
381 to five E(spl) bHLH proteins with Notch-dependent expression (Jennings, Preiss, Delidakis, &
382 Bray, 1994). E(spl) protein expression, and hence Notch signaling, was higher in the
383 morphogenetic furrow in *emc* clones than in wild type cells (Figure 6A). By contrast, E(spl)
384 protein expression was normal in *emc dronc* clones (Figure 6B).
385 To test whether elevated Notch signaling was required to accelerate the morphogenetic
386 furrow in *emc* mutants, we examined *emc psn* double mutant clones. Presenilin (Psn) is the
387 enzymatic component of γ-secretase that releases the intracellular domain of Notch during active

388 Notch signaling, and the *psn* gene is linked to *emc*. Loss of *psn* function leads to a Notch loss of
389 function phenotype (Struhl & Greenwald, 1999; Ye, Lukinova, & Fortini, 1999). Accordingly,
390 *psn* clones lead to a neurogenic phenotype in the eye, without affecting the progression of the
391 morphogenetic furrow (Figure 6C)(Li & Baker, 2001). The position of the morphogenetic
392 furrow was also not affected in *emc psn* clones (Figure 6D). Thus, the furrow was not accelerated
393 in *emc* mutant clones also defective for Notch signaling.
394 These two results together indicated that *emc* mutants promoted Notch signaling in the
395 morphogenetic furrow, acting through caspase signaling on a step prior to γ-secretase cleavage of
396 the intracellular domain of Notch. Accordingly, we decided to check Delta (Dl) protein levels.
397 We found that Dl protein levels were clearly elevated cell-autonomously throughout *emc* clones,
398 both posterior and anterior to the furrow (Figure 7B). Importantly, this includes the region just
399 ahead of the morphogenetic furrow that lacks Delta expression in normal development(Parks,
400 Turner, & Muskavitch, 1995; Baker & Yu, 1998)(Figure 7B). By contrast, levels of Dl protein
401 in *emc dronc* clones and *emc Df(3L)H99* clones were similar to those of wild type controls
402 (Figure 7A,C,D). This indicated that Dl protein is a target of caspases, directly or indirectly.
403 Because Dl activates Notch signaling cell non-autonomously, we wondered whether the
404 effect of *emc* mutant clones was cell-autonomous. We note that, in all the experiments reported
405 here, and in all the previous studies of *emc* mutant clones affecting morphogenetic furrow
406 movement, the morphogenetic furrow is maintained as a continuous groove across the eye disc
407 (Brown et al., 1995; Bhattacharya & Baker, 2011, 2012; Spratford & Kumar, 2013). That is, the
408 advanced front of retinal differentiation within *emc* clones is always smoothly continuous with
409 the normal morphogenetic furrow outside the clones, implying a progressive gradual increase in
410 morphogenetic furrow speed near the lateral edges of *emc* mutant clones (eg Figures 2B, 4B, 4D,
411 5A, 6A). Clones of *Su(H)* null mutants, which act cell-autonomously, provide a contrasting
412 example. Complete loss of *Su(H)* accelerates the morphogenetic furrow due to loss of default
413 Su(H) repression of Notch targets(Li & Baker, 2001). The boundaries of *Su(H)* null clones
414 exhibit a clear discontinuity between the rates of differentiation within and outside the clones
415 (Figure 6E). This difference between *Su(H)* and *emc* mutant clones is consistent with the idea
416 that *emc* affects morphogenetic furrow progression non-autonomously.
417
418 **Specific ommatidial cell fates are regulated by caspases in *emc* mutants**

419

420 Because the general pattern of neurogenesis revealed by pan-neuronal anti-Elav staining
421 appeared so normal in *emc dronc* and *emc Df(3L)H99* clones (Figure 2C,D), we examined
422 whether effects of *emc* on particular retinal cell fates was caspase dependent. Emc is also
423 required for R7 differentiation and for timely onset of cone cell differentiation(Bhattacharya &
424 Baker, 2009), two cell fate decisions that also depend on Notch signaling(Cooper & Bray, 2000;
425 Flores et al., 2000; Tomlinson & Struhl, 2001; Treisman, 2013). These cell fates are normally
426 independent of *da*, but like imaginal disc cell growth and morphogenetic furrow progression,
427 ectopic *da* activity perturbs them in *emc* mutants(Reddy et al.; Brown et al., 1996).
428 Clones of *emc* mutant cells lack R7 photoreceptor cells (Figure 8A,B)(Bhattacharya &
429 Baker, 2009). R7 differentiation was restored to 90% of ommatidia in *emc Df(3L)H99* clones
430 (Figure 8C). As shown before, *emc* mutant clones delayed Cone Cell differentiation by 2-3
431 columns (corresponding to a delay of 3-6 h)(Bhattacharya & Baker, 2009)(Figure 8D,E). We
432 found no delay in cone cell differentiation in most *emc Df(3L)H99* clones (Figure 8F). These
433 results indicated that caspase activity contributes to the R7 and cone cell differentiation defects
434 that are also characteristic of *emc* mutants.
435

436 **Discussion**

437

438 The Inhibitor of DNA binding (Id) proteins are important regulators of
439 differentiation(Massari & Murre, 2000; Ling et al., 2014; Wang & Baker, 2015a; Roschger &
440 Cabrele, 2017; Singh et al., 2022). They are well known to antagonize proneural basic helix-
441 loop-helix (bHLH) proteins (Benezra et al., 1990; Ellis et al., 1990; Garrell & Modolell, 1990;
442 Cabrera et al., 1994; Ellis, 1994; Norton, 2000). It has been uncertain whether this is their only
443 function, as in *Drosophila* it is clear that *emc* mutations affect processes that are independent of
444 proneural genes. Here, we report that multiple effects of *emc* mutations that occur independently
445 of proneural bHLH genes, and are due to the loss of restraint on *da* function in *emc* mutant cells,
446 are caused by caspase-dependent non-apoptotic processes that result from reduced expression of
447 Diap1 protein.
448 One known effect of *emc* is that it restrains the *Drosophila* E protein Da. Da is expressed
449 ubiquitously and is the obligate heterodimer partner of proneural bHLH proteins in neurogenesis.

450 In undifferentiated progenitor cells, most or all Da is thought to be sequestered in inactive
451 heterodimers with Emc(Li & Baker, 2018). In *emc* mutant cells, Da levels rise and become
452 functional, potentially as homodimers(Bhattacharya & Baker, 2011).
453 In the context of imaginal disc cell growth, *emc* mutant cells experience *da*-dependent
454 over-expression of the *ex* gene(Wang & Baker, 2015b, 2018). Although most study of *ex* has
455 focused on its role in growth control through the SHW pathway, *ex* was recently shown to
456 influence patterning through Yki-dependent transcription of *diap1*, an important regulator of cell
457 death pathways. This was in the developing thorax, where *ex* mutations affect bristle patterning
458 through *diap1* and a non-apoptotic effect of caspases on Wg signaling(Wang & Baker, 2019).
459 This observation led us to explore whether aspects of the *emc* phenotype could reflect reduced
460 *diap1* expression and elevated caspase activity.
461 Remarkably, we found that all four features of the *emc* phenotype we examined depended
462 on the caspase-mediated cell death pathway. The normal growth of imaginal disc cells, normal
463 speed of the morphogenetic furrow, specification of R7 photoreceptor cells, and timing of non-
464 neuronal cone cell development were all restored when caspase activation was prevented, which
465 was achieved by inactivating the initiator caspase Dronc, deleting the proapoptotic *rpr*, *grim*, and
466 *hid* genes, over-expressing *diap1*, or over-expressing baculovirus p35. These appeared to be
467 non-apoptotic effects, because no elevation in apoptosis was apparent in *emc* mutant cells,
468 because generating apoptosis by another means did not mimic the effects, and because the effects
469 were mediated by elevated Dl protein expression in cells that were not apoptotic. They appeared
470 to be effects of caspase activity, because they depended in part on *dronc*, an initiator caspase that
471 cleaves and activates effector caspases, because they were suppressed by baculovirus p35, a
472 caspase inhibitor that is a caspase pseudo-substrate, and because they were suppressed by Diap1,
473 a ubiquitin ligase that inhibits caspases and targets them for degradation. The effects may
474 depend on the full caspase cascade of initiator and effector caspases, because sensitivity to p35
475 indicates that caspases other than Dronc are necessary, and because mutating dronc alone gave
476 lesser degrees of rescue than deleting *rpr*, *grim*, and *hid*. This is consistent with many other
477 studies that describe the pathways for apoptotic and non-apoptotic caspase functions as
478 similar(Kanuka et al., 2005; Kuranaga & Miura, 2007; Aram et al., 2017; Nakajima & Kuranaga,
479 2017; Baena-Lopez et al., 2018; Su, 2020; Colon-Plaza & Su, 2022).

480 Whereas non-apoptotic caspase activity promotes Wg signaling during specification of
481 thoracic bristles(Kanuka et al., 2005), in the *Drosophila* eye the non-apoptotic caspase target was
482 Notch signaling, due to elevated Delta protein levels. We do not know whether Delta is the direct
483 caspase target. The Delta protein sequence contains multiple predicted caspase target sites, as do
484 many proteins (Wang et al., 2014). Only one candidate site lies in the intracellular domain,
485 where it would potentially be accessible to caspases (Figure 9B). Truncation of the Dl
486 intracellular domain is usually associated with loss of Dl function, not stabilization and enhanced
487 function, however (Daskalaki et al., 2011). Another possibility is that a regulator of Dl
488 expression or stability and function is the direct caspase target.
489 Notably, *emc* mutations accelerate the morphogenetic furrow by enhancing Notch
490 signaling, apparently cell-autonomously, but inhibit R7 and cone cell differentiation through
491 cell-autonomously reduced N signaling(Reddy et al.; Bhattacharya & Baker, 2009). These
492 contrasts may be explained through the dual functions of the Notch ligand Delta in trans-
493 activation and in cis-inhibition (Micchelli, Rulifson, & Blair, 1997; Jacobsen, Brennan,
494 Martinez-Arias, & Muskavitch, 1998; Li & Baker, 2004; Bray, 2016). The eye disc region ahead
495 of the morphogenetic furrow lacks Delta expression (Parks et al., 1995; Baker & Yu, 1998).
496 Ectopic Dl expression here is sufficient to activate N non-autonomously and drive
497 morphogenetic furrow progression (Baonza & Freeman, 2001a; Li & Baker, 2001). Within the
498 R7 equivalence group, Delta is expressed early in R1 and R6 photoreceptor precursors,
499 protecting them from N activation through cis-inhibition, and establishing the distinction
500 between R1,6 and R7 precursor cells (Miller, Lyons, & Herman, 2009). Ectopic Dl expression
501 posterior to the morphogenetic furrow has cis-inhibitory effect. Elevated Dl levels within *emc*
502 mutant clones may render potential R7 and cone cell precursors cell-autonomously resistant to N
503 activation, as normally seen in R1/6 precursor cells.
504 A previous study suggested that *emc* mutations might affect Hh signaling (Spratford &
505 Kumar, 2013). Our data point much more clearly to an effect on Notch signaling. Although the
506 Hh target Ci155 accumulates in *emc* mutant cells, increased Hh signaling is not the only possible
507 cause of this. Ci155 is cytoplasmic, and thought to be only a precursor for a labile nuclear
508 activator molecule(Ohlmeyer & Kalderon, 1998). Preventing activation and nuclear
509 translocation of Ci155 by mutating the kinase *fused* also leads to Ci155 accumulation, without
510 activating Hh signaling. Presumably Ci155 accumulates because it is more stable than its

511 activated derivative(Ohlmeyer & Kalderon, 1998). Significantly, *emc* mutant cells have been
512 reported to over-express the *fused* antagonist *su(fu)*, providing a potential alternative explanation
513 of Ci155 accumulation in *emc* mutant cells(Spratford & Kumar, 2013). Analyzing *emc ci* double
514 mutant cells suggested that *ci* was not required to accelerate the morphogenetic furrow in *emc*
515 mutant clones.
516 Da protein binds to and potentially regulates hundreds of genes throughout the
517 *Drosophila* genome(Li et al., 2008). Accordingly, Da activity in *emc* mutant cells might be
518 expected to lead to non-specific and pleiotropic effects. Contrary to this expectation, multiple
519 aspects of proneural bHLH-independent *emc* mutant phenotypes have a simple common basis, ie
520 reduced *diap1* expression and elevated caspase activity. Remarkably, mutating *emc* may be the
521 most general way to activate non-apoptotic caspase activities yet discovered.
522
523
524
525
526
527
528
529
530
531
532
533
534
535
536
537
538
539

540 **Figure Legends**

Figure 1

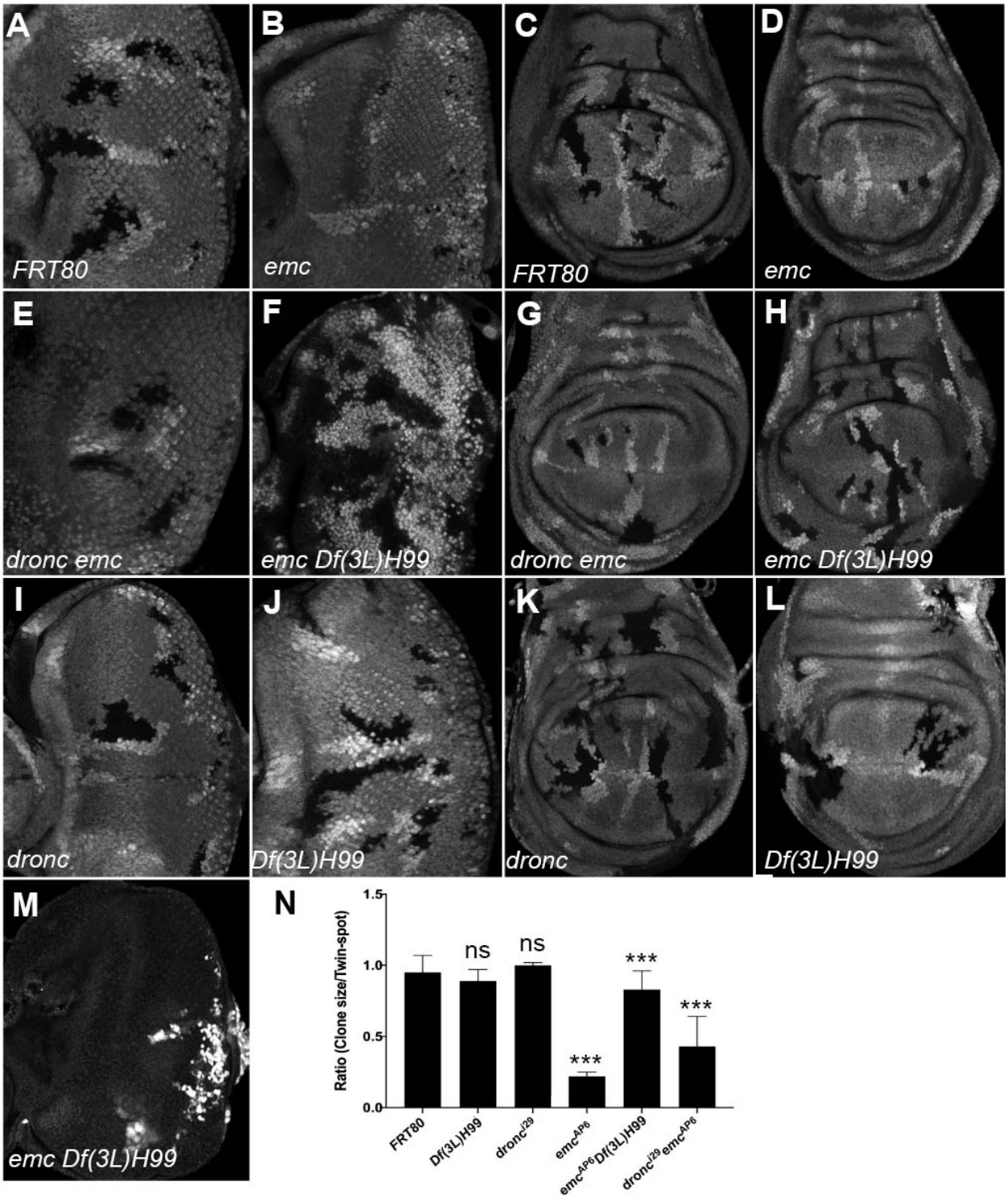

541

542 **Figure 1: *Df(3L)H99* rescues growth of *emc* mutant**

543 (A-L) Control and mutant clones in eye and wing imaginal disc were induced at the end of first
544 instar and are associated with sibling twin-spot clones marked by two copies of the GFP marker
545 (brighter grey) that serves as internal control for growth. Clones are labeled by the absence of
546 GFP. (M) *emc H99* clones induced in the minute background (N) Quantification of the ratio of
547 clone size to twin-spot measured in wing imaginal discs and standard deviations. After log-
548 transformation of clone/twin-spot ratios to ensure normality, one way ANOVA rejected the null
549 hypothesis that these results are the same ($p=2.57 \times 10^{-10}$). The Holm correction for multiple
550 comparison was used to identify significant differences between all pairs of samples. Whereas
551 clone/twin-spot ratios for *Df(3L)H99* and *dronc*^{i29} did not differ significantly from the FRT80
552 control ($p>0.05$), that for *emc* homozygous clones was significantly different ($p=4.95 \times 10^{-8}$).
553 Ratios for both *emc Df(3L)H99* and *emc dronc* clones differed significantly from *emc* clones
554 ($p=2.19 \times 10^{-8}$ and 4.89×10^{-4}, respectively). Clone/twin-spot ratios for *emc dronc* clones also
555 differed significantly from *dronc* clones ($p=0.044$) and from *Df(3L)H99* clones ($p=0.048$).
556 For columns 2-4, *** denotes significant difference from the FRT80 control ($p<0.001$), NS
557 denotes no significant difference. For columns 5-6, *** denotes significant difference from the
558 *emc* clones.
559 Genotypes: (A and C) *ywhsF;;FRT80/[UbiGFP]FRT80* (B and D) *ywhsF;;emc*^{AP6}*FRT80/[Ubi-*
560 *GFP]FRT80* (E and G) *ywhsF;;dronc*^{i29}*emc*^{AP6} em*FRT80/[UbiGFP]FRT80* (F and H)
561 *ywhsF;;emc*^{AP6} *Df(3L)H99 FRT80/[UbiGFP]FRT80* (I and K) *ywhsF;;dronc*^{i29}
562 *FRT80/[UbiGFP]FRT80* (J and L) *ywhsF;;Df(3L)H99FRT80/[UbiGFP]FRT80* (M) *ywhsF;*
563 *emc*^{AP6} *Df(3L)H99 FRT80/[UbiGFP] M(3)67C FRT80*.
564

Figure 2

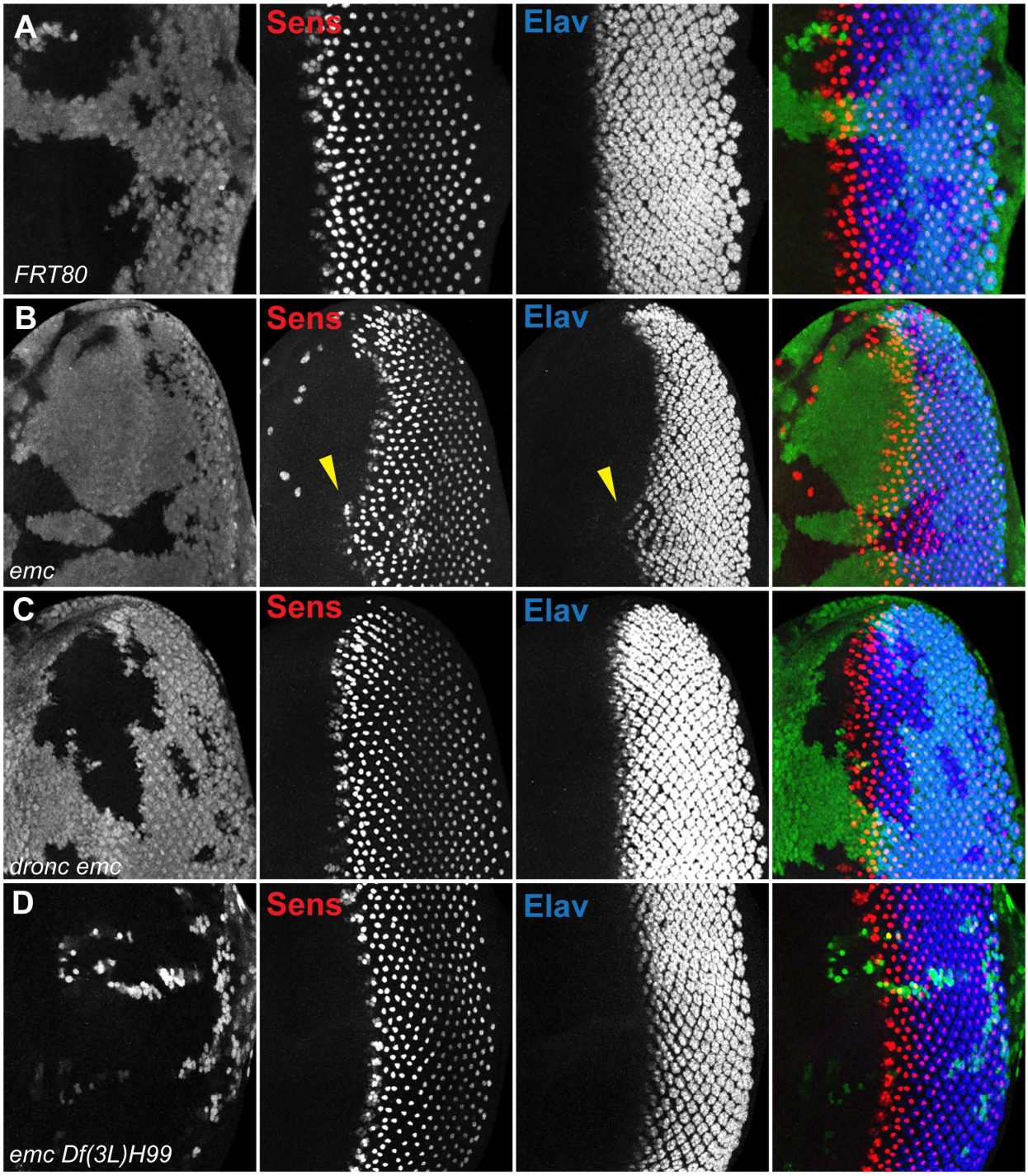

Figure 2: Morphogenetic furrow progression is affected by cell death pathways

In all panels, the differentiating neurons are marked by Elav (in blue), and mutant cells are identified by the absence of GFP expression (in green). A) The wave of retinal differentiation from posterior to anterior (right to left), marked here by Senseless expression in R8

570 photoreceptor cells (red) is normal in FRT80 control clones. B) *emc* null cell lacking GFP shows
571 acceleration of retinal differentiation marked by yellow arrow. C) In contrast, retinal
572 differentiation proceeds at the same pace in *emc dronc* double mutant clones as in nearby wild
573 type regions in 75% of the eye discs. D) *emc H99* double mutants show a stronger suppression of
574 the acceleration of retinal differentiation (compare panel B). Genotypes: (A)
575 *ywhsF;;FRT80/[UbiGFP] M(3)67C FRT80* (B) *ywhsF;;emc*^{AP6}*FRT80/[Ubi-GFP] M(3)67C*
576 *FRT80* (C) *ywhsF;;dronc*^{i29}*emc*^{AP6} *FRT80/[UbiGFP] M(3)67C FRT80* (n=12)(D) *ywhsF;;emc*^{AP6}
577 *Df(3L)H99 FRT80/[UbiGFP] M(3)67C FRT80*.

Figure 3

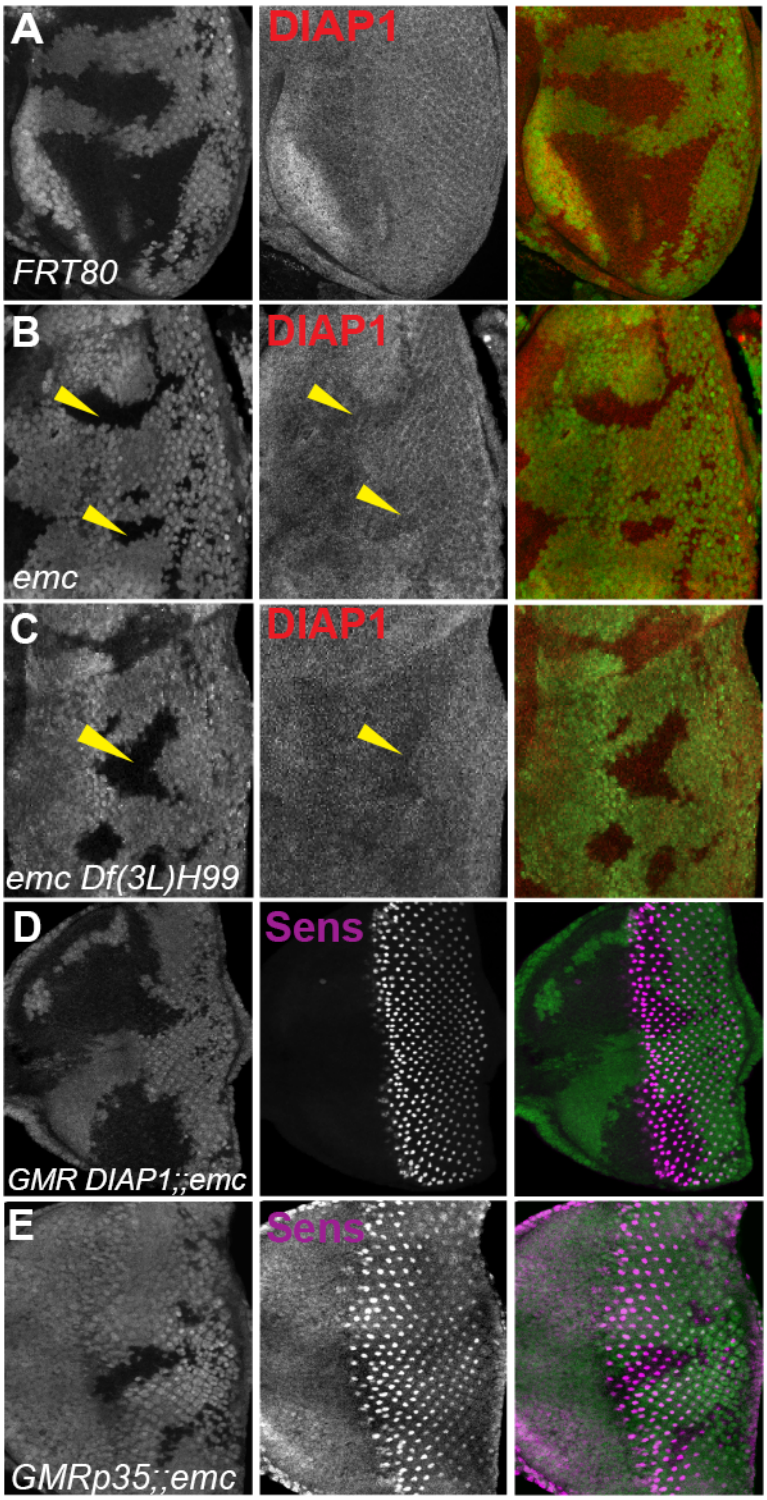

578

579 **Figure 3: Diap1 expression and function in *emc* mutant clones**

580 In mosaic eye discs with (A) FRT80 clones, there is no change in Diap1 levels within and

581 outside the clone. However, both (B) *emc* mutant clones and (C) *emc H99* clones show reduced

582 Diap1 levels. (D) In GMR-DIAP1 eye disc mutant for emc furrow progression is normal and is
583 marked by Senseless staining. Similarly, in GMR-p35 eye disc mutant for emc also show normal
584 furrow progression (E). Genotypes: (A) *ywhsF;;FRT80/[UbiGFP] M(3)67C FRT80* (B)
585 *ywhsF;;emc^{AP6}FRT80/[Ubi-GFP] M(3)67C FRT80* (C) *ywhsF;;emc^{AP6} Df(3L)H99*
586 *FRT80/[UbiGFP] M(3)67C FRT80* (D) ywhsF/GMR-DIAP1;;*emc^{AP6}FRT80/[Ubi-GFP]*
587 *M(3)67C FRT80*. (E) ywhsF/GMR-p35;;*emc^{AP6}FRT80/[Ubi-GFP] M(3)67C FRT80*.
588

Figure 4

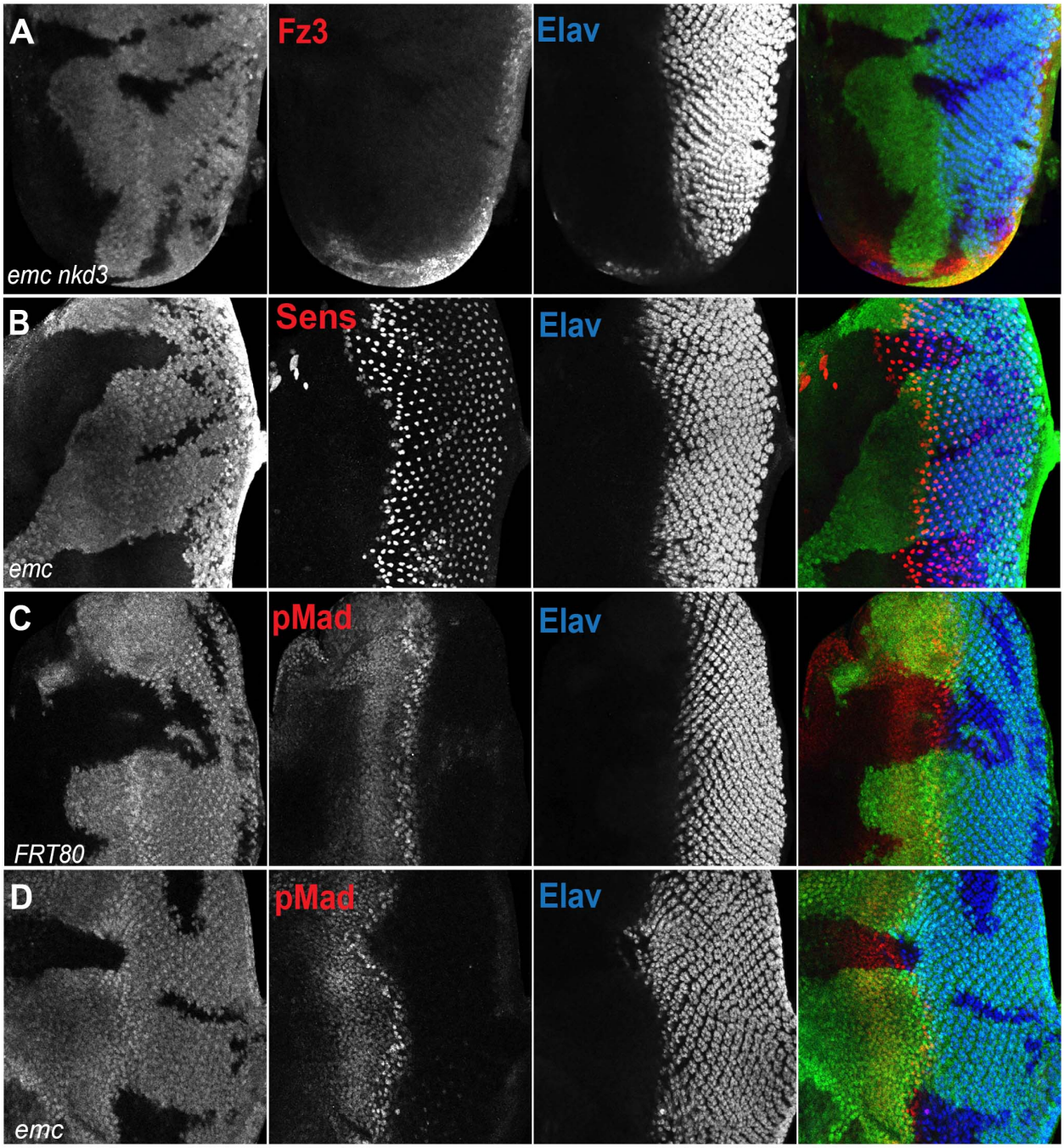

589

590 **Figure 4: Wingless and Dpp signaling are not caspase targets**

591 (A) No reduction in the Wg signaling reporter Fz3-RFP was detectable in emc clones. See
592 Figure 4 Figure Supplement 1 for Fz3-RFP expression in the wild type. (B) Retinal
593 differentiation is accelerated in *emc nkd*^{3} double mutant clones like in *emc* clones. Senseless
594 expression in R8 photoreceptor cells and Elav staining in differentiating photoreceptors are

595 shown. (C) p-Mad accumulates around the morphogenetic furrow in eye discs containing control
596 clones(Vrailas & Moses, 2006; Firth, Bhattacharya, & Baker, 2010) (E) Except for the advanced
597 progression, p-Mad levels were unchanged in *emc* clones. Genotypes: (A) Fz3-RFP/+;
598 *emc^{AP6}FRT80/[Ubi-GFP] M(3)67C FRT80* (B) *ywhsF;;emc^{AP6}nkd^{3}FRT80/[Ubi-GFP] M(3)67C*
599 *FRT80* (C) *ywhsF;;FRT80/[UbiGFP] M(3)67C FRT80* (D) *ywhsF;;emc^{AP6}FRT80/[Ubi-GFP]*
600 *M(3)67C FRT80***.**
601

Figure 5

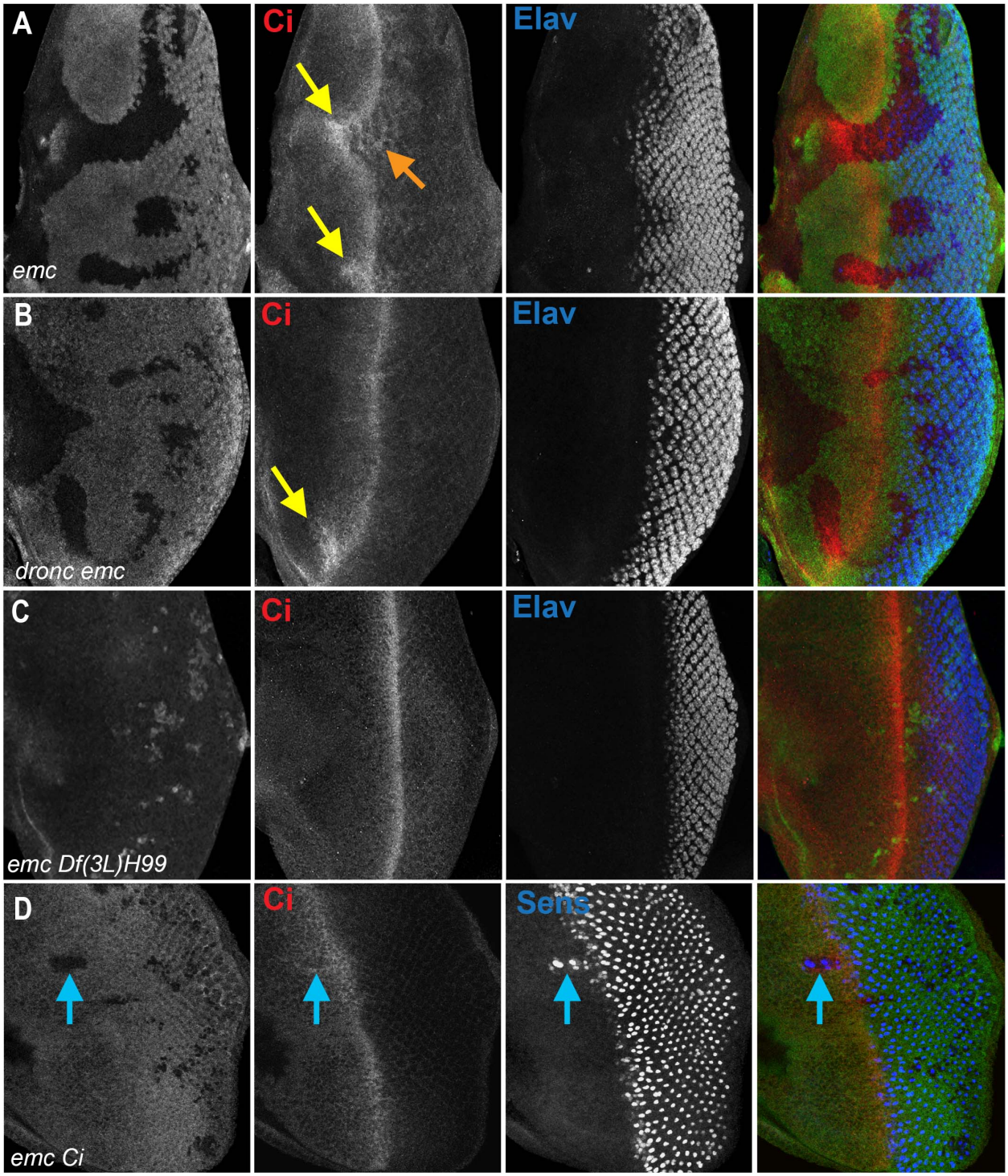

Figure 5: Ci expression and function in *emc* mutant clones

A) Ci is elevated within *emc* mutant cells (yellow arrows). This was also true posterior to the morphogenetic furrow (orange arrow) B) Higher Ci was also seen in *emc dronc* mutant cells, even when the morphogenetic furrow progressed normally, as indicated by Elav staining. C) Ci

607 levels were completely normal in *emc H99* clones. D) *emc* and *ci* doubly-mutant clone lacking
608 GFP shows accelerated retinal differentiation (blue arrow). Genotypes: (A)
609 *ywhsF;;emc^{AP6}FRT80/[Ubi-GFP] M(3)67C FRT80* (B) *ywhsF;;dronc^{i29}emc^{AP6}*
610 *FRT80/[UbiGFP] M(3)67C FRT80* (C) *ywhsF;;emc^{AP6} Df(3L)H99 FRT80/[UbiGFP] M(3)67C*
611 *FRT80* (D) *ywhsF;;emc^{AP6}FRT80/[Ubi-GFP] ci^{+} M(3)67C FRT80;ci[94]/ci[94].*
612

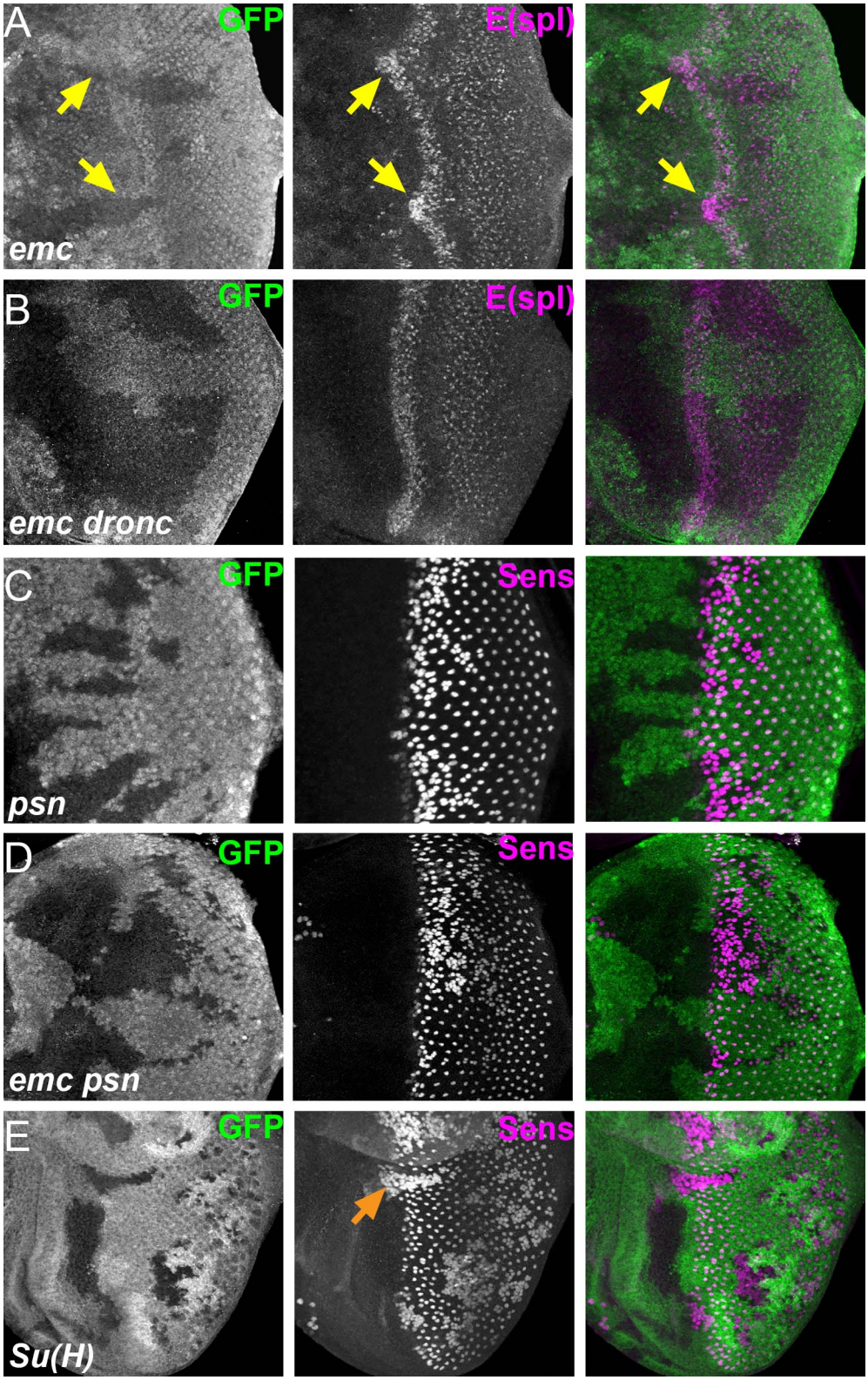

Figure 6: Non-apoptotic caspase signaling targets Notch pathway by promoting Dl expression

616 (A) E(spl), an important N target for lateral inhibition, is elevated in the morphogenetic furrow
617 region of *emc* clones (yellow arrows). (B) *emc dronc* clones have normal levels of E(spl) protein.
618 (C) Senseless staining shows a neurogenic phenotype in *psn* mutant clones, due to reduced Notch
619 signaling. Morphogenetic furrow progression is unaffected. (D) A neurogenic phenotype was
620 also observed in *emc psn* clones, along with normal furrow progression. (E) *Su(H)* mutant clones
621 identified by absence of GFP labeling show a strong neurogenic phenotype as well as advanced
622 retinal differentiation (orange arrow) (Li & Baker, 2001). The cell-autonomous effect results in
623 a discontinuity at the borders of *Su(H)* clones, where differentiation outside the clones lags that
624 within clones (orange arrow) Genotypes: (A) *ywhsF;;emc*^{AP6} *FRT80/[Ubi-GFP] M(3)67C*
625 *FRT80* (B) *ywhsF;; dronc*^{i29}*emc*^{AP6} *FRT80/[UbiGFP] M(3)67C FRT80* (C) *ywhsF/+;;psn*^{V1}
626 *FRT80/[Ubi-GFP]M(3)67CFRT80* (D) *ywhsF/+;; emc*^{AP6} *psn*^{V1} *FRT80/[Ubi-*
627 *GFP]M(3)67CFRT80* ((E) *ywhsF; Su(H)*^{D47}FRT40/FRT40*[UbiGFP]*.
628

Figure 7

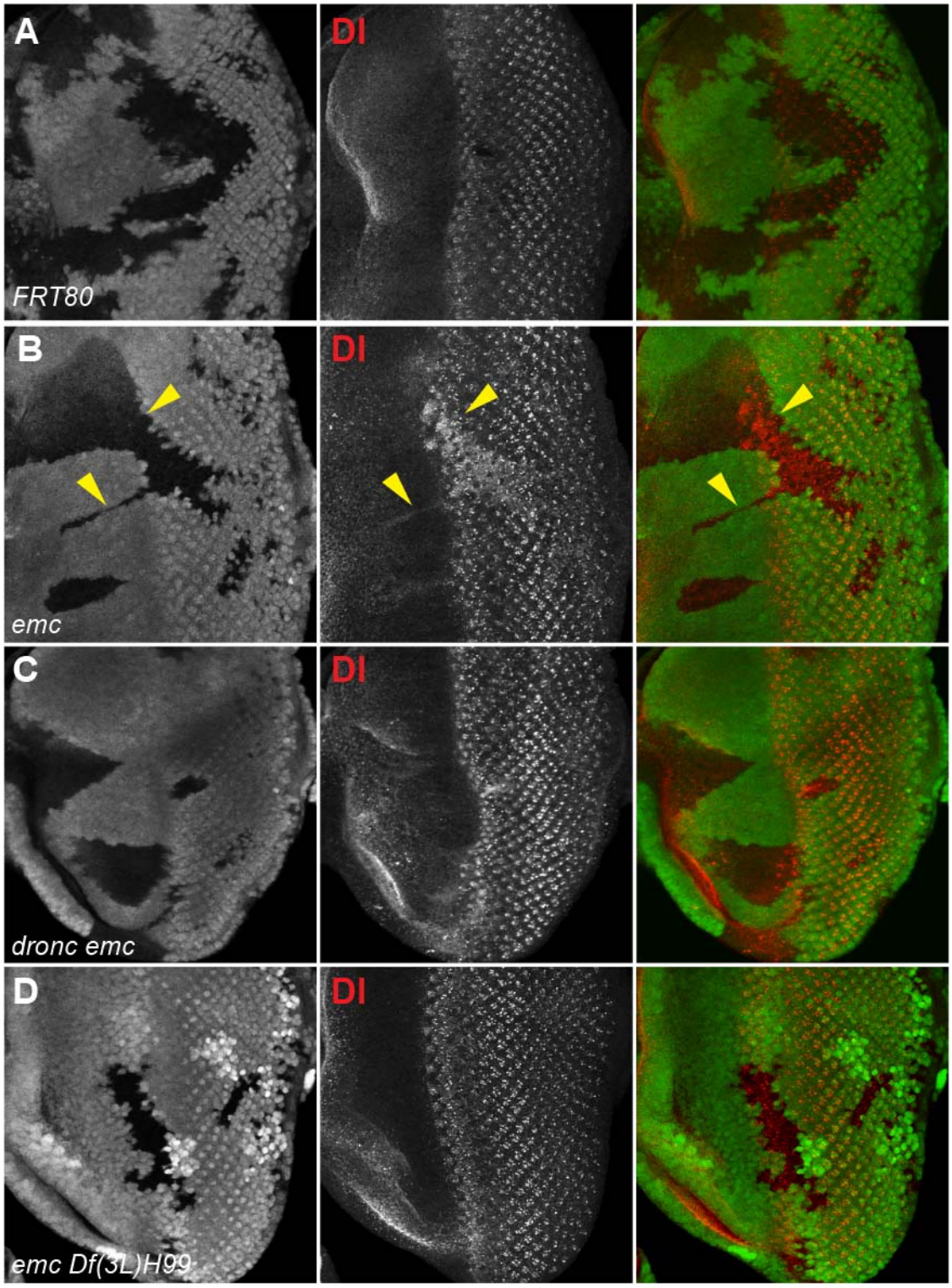

Figure 7: Caspase regulation of Delta levels

631 (A) Normal levels of Delta protein are seen in FRT80 clones as compared to elevated Delta
632 levels in (B) *emc* clones whereas that phenotype is reversed in (D) *emc H99* clones. However, as
633 seen in (C) *dronc emc* clones show high Delta levels. Genotypes: (A) *ywhsF;;FRT80/[UbiGFP]*
634 *M(3)67C FRT80* (B) *ywhsF;;emc*^{AP6}*FRT80/[Ubi-GFP] M(3)67C FRT80* (C)
635 *ywhsF;;dronc*^{i29}*emc*^{AP6} *FRT80/[UbiGFP] M(3)67C FRT80* (D) *ywhsF;;emc*^{AP6} *Df(3L)H99*
636 *FRT80/[UbiGFP]FRT80.*
637

Figure 8

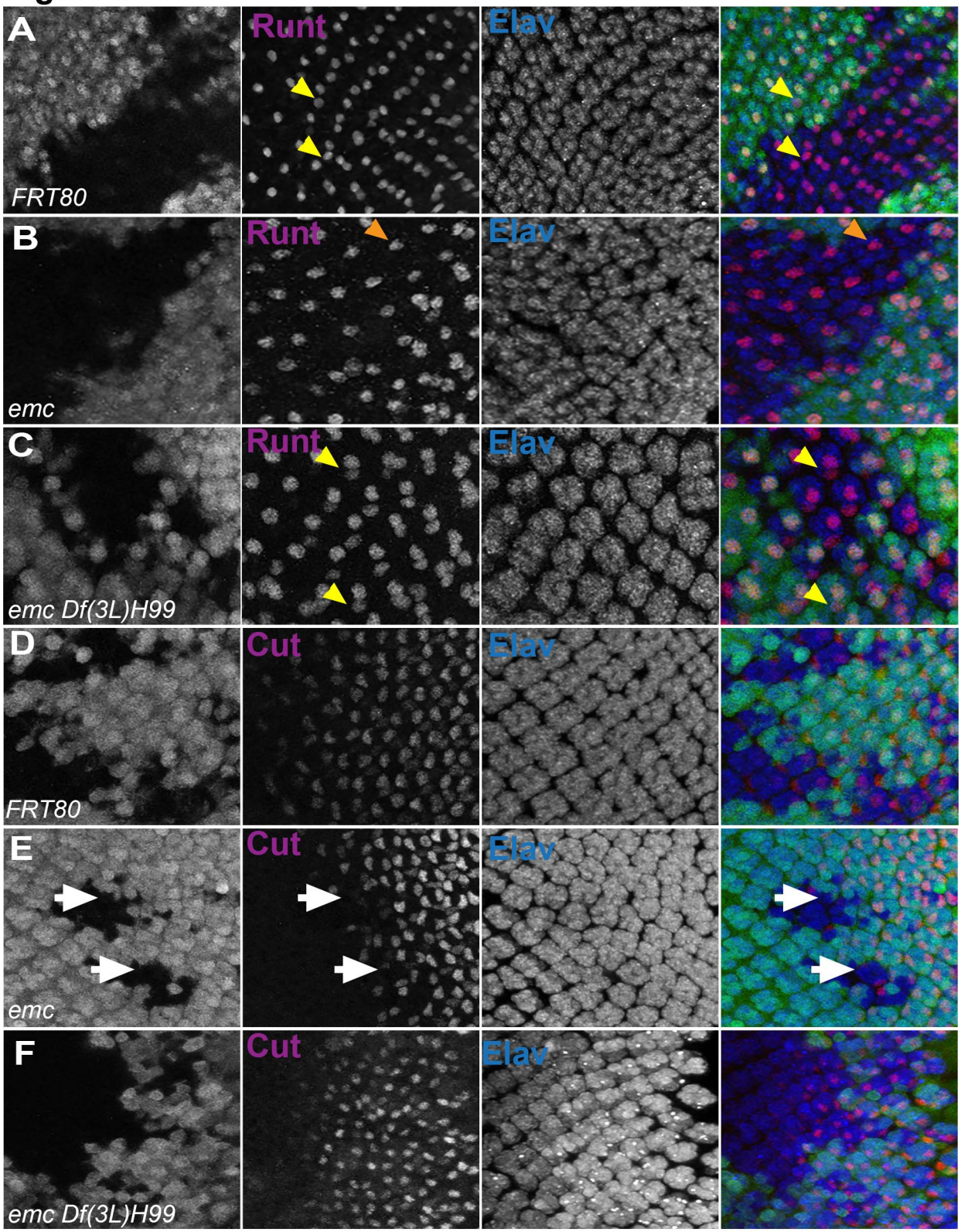

638

639 **Figure 8: Caspases contribute to R7 photoreceptor and cone cell defects in *emc* mutants**

640 In all panels *emc* mutant cells are marked by the absence of GFP expression (in green) and
641 photoreceptor neurons are marked by Elav in blue. (A) Runt (in red) is expressed in R7 and R8
642 (yellow arrowhead) photoreceptor cells inside and outside the clone in FRT80 controls. (B)
643 Inside *emc* clone, Runt expression is lost from R7 cells, while expression in R8 cells remains
644 unaffected (red arrow). (C) However, inside the *emc H99* clones, Runt is expressed in both R7
645 and R8 cells. (D) Cut (in red) is expressed in cone cells in FRT80 controls. (E) Inside *emc* clone,
646 cut is delayed. (F) However, inside the *emc H99* clones, cut staining is not delayed. Genotypes:
647 (A, D) *ywhsF;;FRT80/[UbiGFP] M(3)67C FRT80* (B, E) *ywhsF;;emc*^{AP6}*FRT80/[Ubi-GFP]*
648 *M(3)67C FRT80* (C, F) *ywhsF;;emc*^{AP6} *Df(3L)H99 FRT80/[UbiGFP] M(3)67C FRT80.*
649

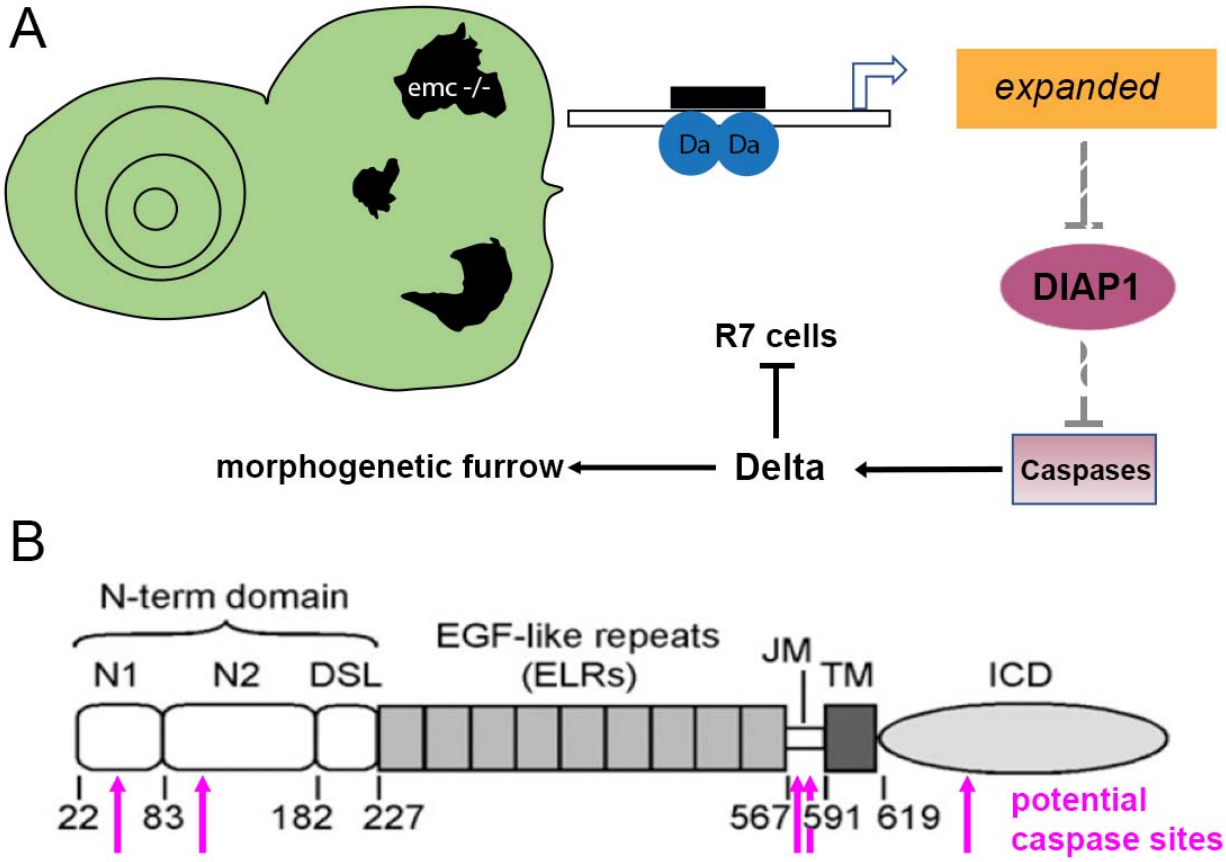

650

651 **Figure 9: Model of *emc* effects on *Drosophila* eye development.** A) Loss of *emc* allows Da
652 protein to form heterodimers and activate *ex* transcription, increasing SHW pathway activity.
653 SHW activity reduces DIAP1 expression, thereby derepressing caspase activity. In the eye, non-
654 apoptotic caspase activity increases expression of the Notch ligand Delta. Elevated Delta
655 expression accelerates morphogenetic furrow progression, while cis-inhibiting Notch signaling

656 posterior to the morphogenetic furrow, inhibiting R7 cell specification and cone-cell
657 differentiation. B) Like many proteins, Delta has multiple potential caspase cleavage sites, here
658 predicted suing Cascleave 2.0 (Wang et al., 2014). None are high-confidence predictions and
659 only one is in the intracellular domain where caspase access is plausible (position 675, predicted
660 score 0.647). The intracellular domain is required for Delta signaling. Cleavage at position 675
661 would remove the main ubiquitylation site required for signaling, as well as the binding site for
662 *mindbomb*, so is not anticipated to enhance signaling activity (Daskalaki et al., 2011).
663

Figure 2 figure supplement

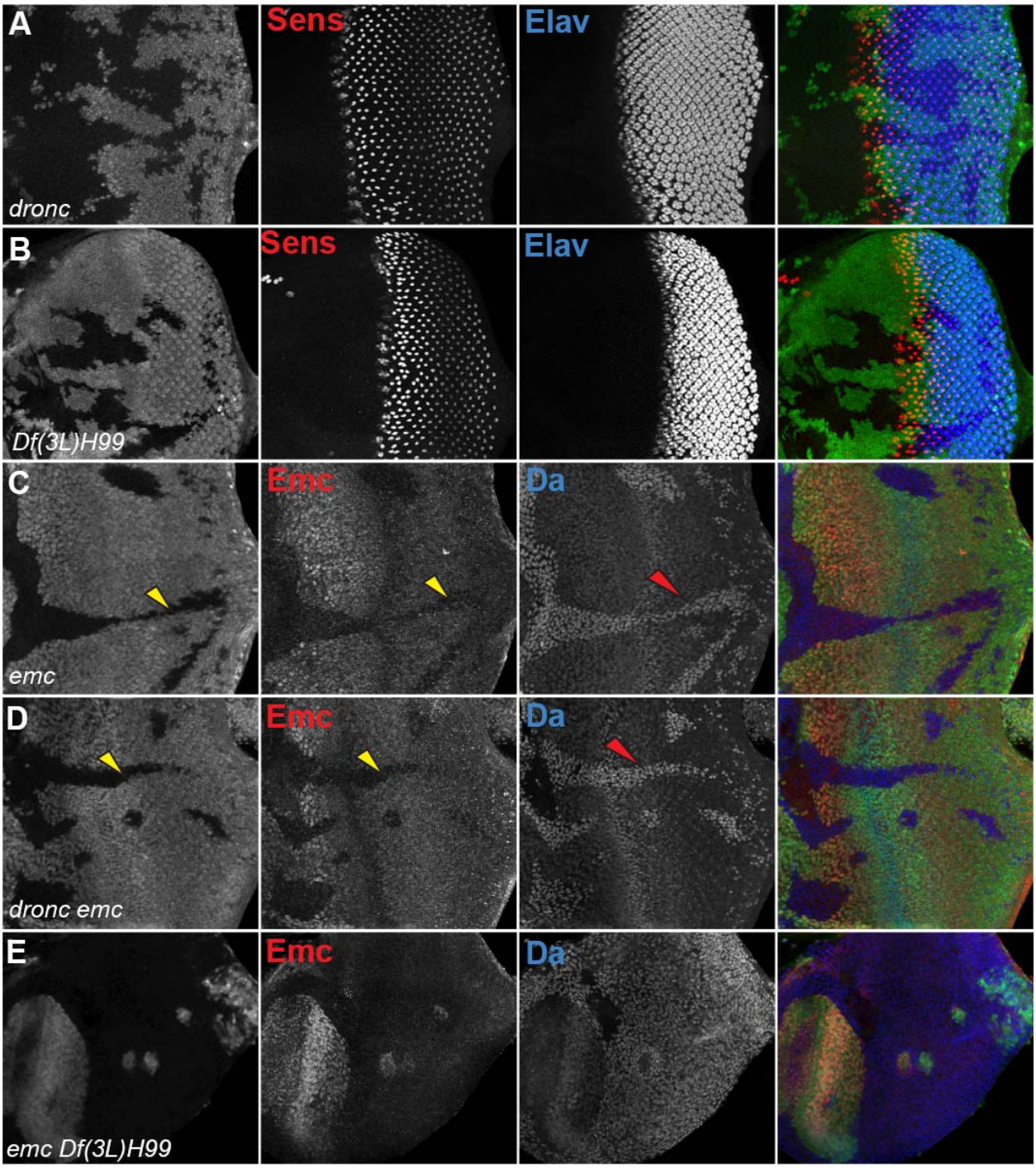

Figure 2 Figure Supplement 1: Morphogenetic furrow progression in *emc* mutant cells

In eye imaginal discs, normal furrow progression was observed in (A) *dronc* $^{-/-}$ and (B) *Df(3L)H99* homozygous clones, indicated by Senseless and Elav staining. Homozygous mutant clones of *emc*$^{-/-}$ (C) lacking GFP expression, have no Emc staining (yellow arrowhead) and

669 higher Da (red arrowhead). At the morphogenetic furrow as shown by yellow arrow, Emc
670 expression goes down and Da goes up. Similar results were observed in (D) *dronc*$^{-/-}$ *emc*$^{-/-}$ clones
671 and (E) *emc*$^{-/-}$ *Df(3L) H99* $^{-/-}$ clones confirm that these are *emc* null clones. Genotypes: (A)
672 *ywhsF;;dronc*^{i29}*FRT80/[UbiGFP] M(3)67C FRT80* (B) *ywhsF;; Df(3L)H99 FRT80/[UbiGFP]*
673 *M(3)67C FRT80*. (C) *ywhsF;;emc*^{AP6}*FRT80/[Ubi-GFP] M(3)67C FRT80* (D)
674 *ywhsF;;dronc*^{i29}*emc*^{AP6} *FRT80/[UbiGFP] M(3)67C FRT80* (E) *ywhsF;;emc*^{AP6} *Df(3L)H99*
675 *FRT80/[UbiGFP] M(3)67C FRT80*.
676

Figure 2 Figure Supplement 2

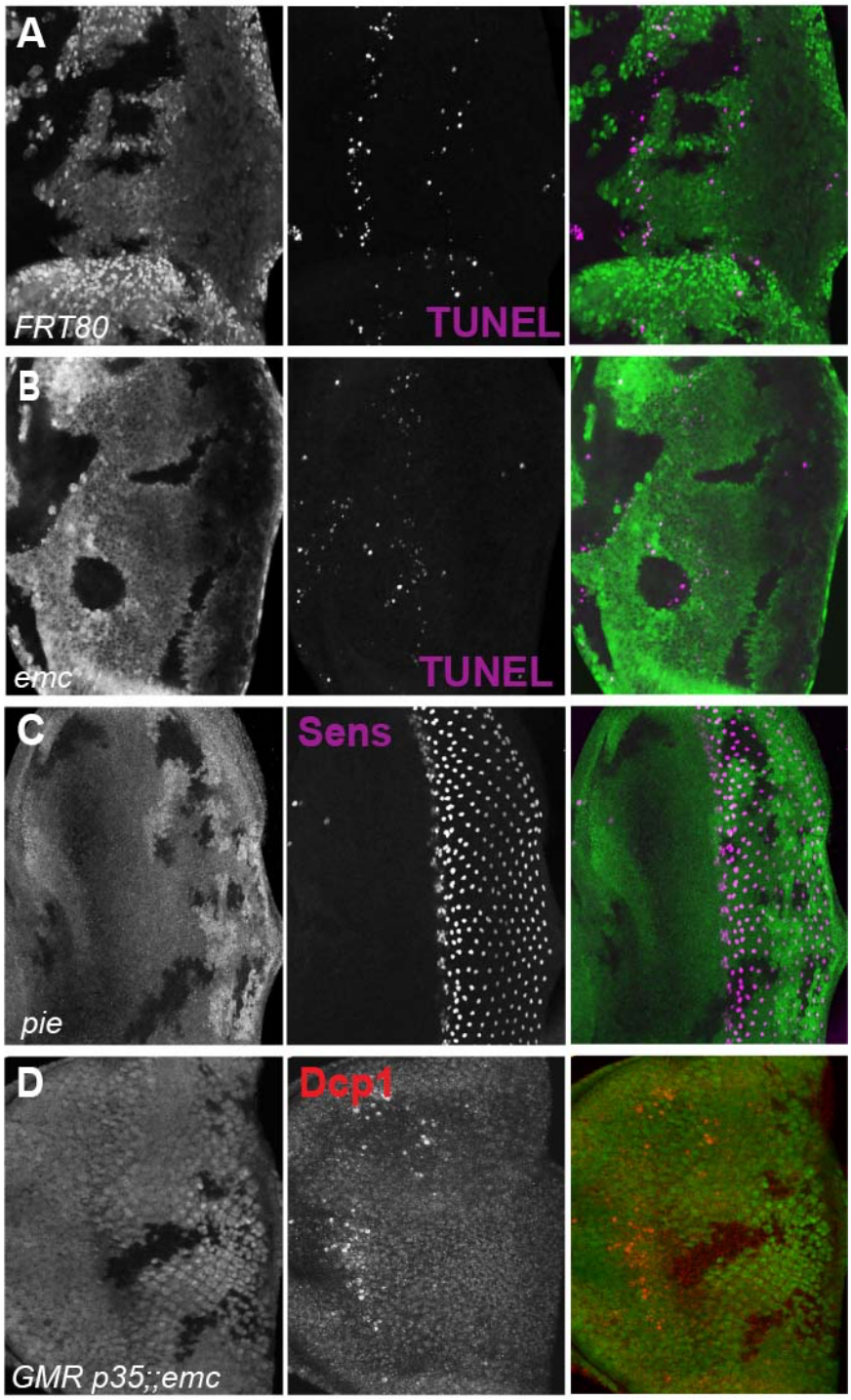

677

678 **Figure 2 Figure Supplement 2: Apoptosis and furrow progression** Representative images of
679 eye imaginal discs stained for TUNEL (A) *ywhsF;;FRT80/[UbiGFP] M(3)67C FRT80* (B)
680 *ywhsF;;emc*^{AP6}*FRT80/[Ubi-GFP] M(3)67C FRT80*. In (C) *pie*^{EB3} homozygous clones, furrow
681 progression occurs at normal speed marked by Senseless staining in R8 photoreceptors. (D) In

682 GMR-p35 eye disc mutant for emc also show lack of Dcp1staining. Genotypes: (A)
683 *ywhsF;;FRT80/[UbiGFP] M(3)67C FRT80* (B) *ywhsF;;emc^{AP6}FRT80/[Ubi-GFP] M(3)67C*
684 *FRT80* (C) ywhsF/+; *pie^{EB3}FRT40/FRT40Alz*. (D) ywhsF/GMR-p35;;*emc^{AP6}FRT80/[Ubi-GFP]*
685 *M(3)67C FRT80*.
686

Figure 4 figure supplement 1

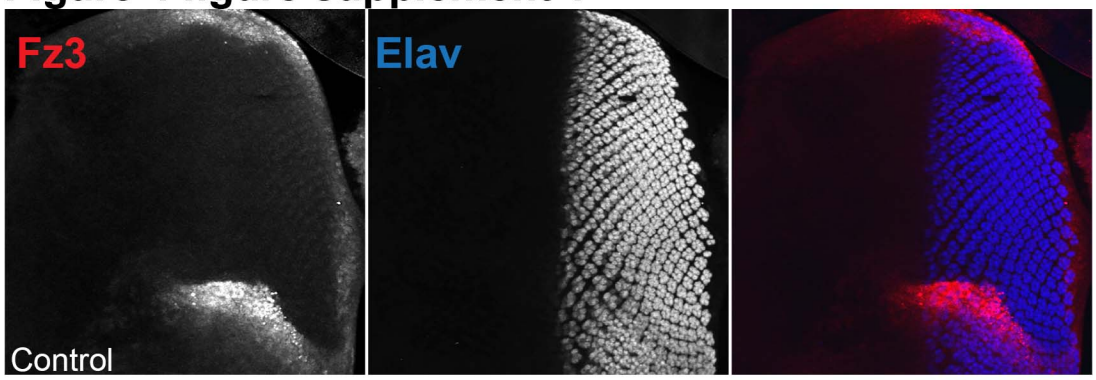

687

688 **Figure 4 Figure Supplement 1:** Fz3-RFP/+ eye disc showing RFP and Elav staining.
689

Figure 5 figure supplement 1

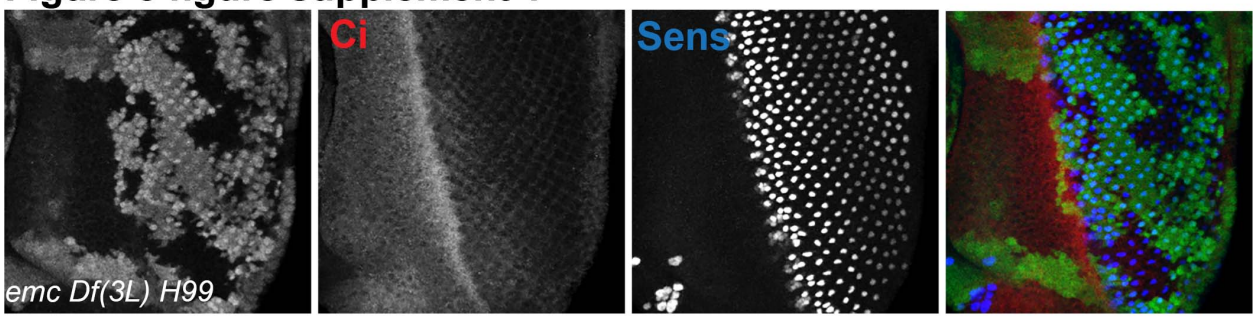

690

691 **Figure 5 Figure Supplement 1: Ci155 levels when cell death pathways are blocked**
692 Representative image of eye imaginal disc in *emc H99* clones in the non-Minute background,
693 showing similar areas inside and outside clones. Genotype: *ywhsF;; emc^{AP6} Df(3L)H99*
694 *FRT80/[UbiGFP]FRT80*
695

Figure 5 Figure Supplement 2

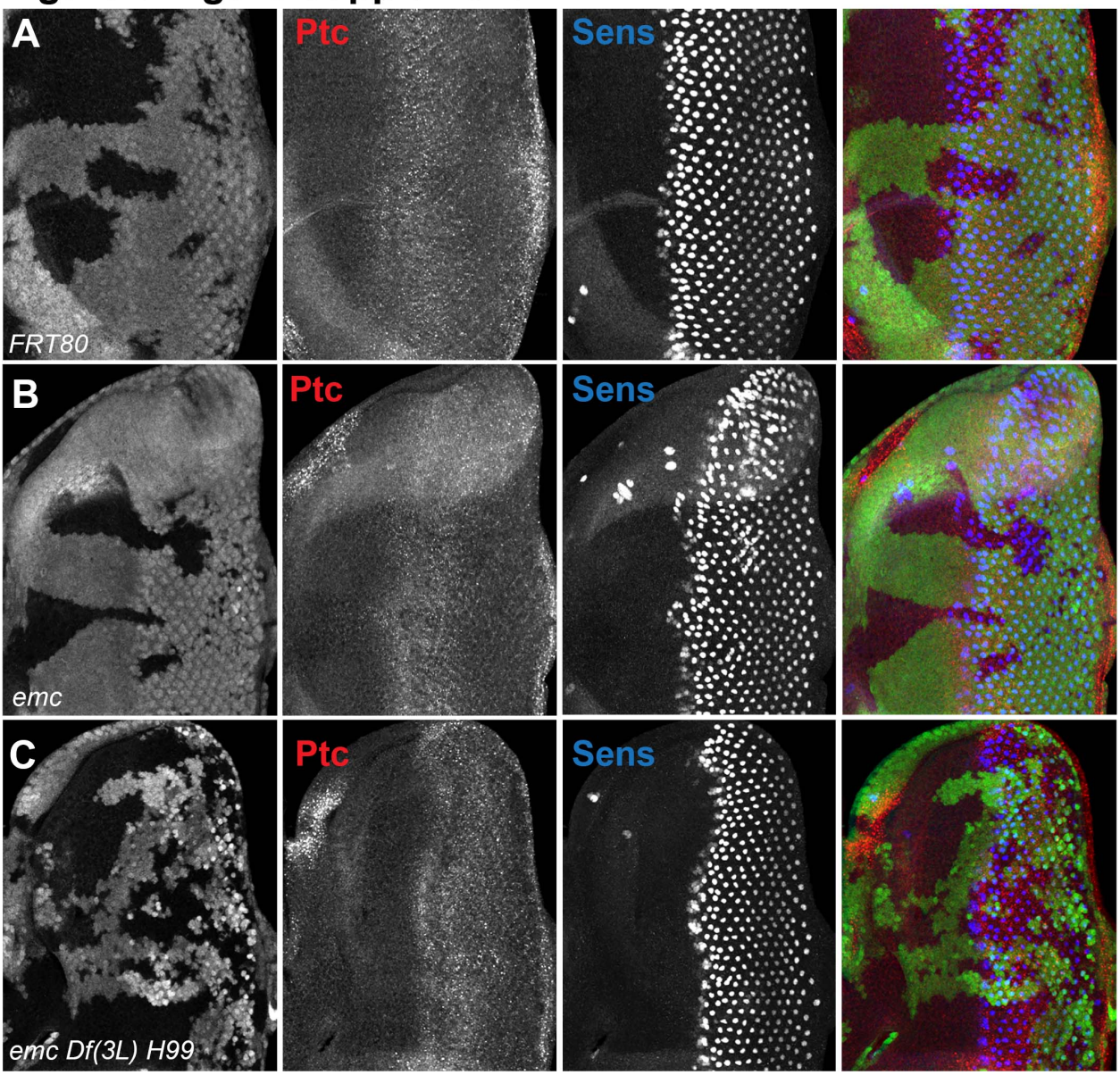

696

697 **Figure 5 Figure Supplement 2: Patched staining in emc mutants**

698 (A) *ywhsF;;FRT80/[UbiGFP] M(3)67C FRT80* (B) *ywhsF;;emc^{AP6}FRT80/[Ubi-GFP] M(3)67C*

699 *FRT80* (C) *ywhsF;;emc^{AP6} Df(3L)H99 FRT80/[UbiGFP] M(3)67C FRT8.*

700

701

References

Adam, J. C., & Montell, D. J. (2004). A role for extra macrochaetae downstream of Notch in follicle cell differentiation. *Development, 131*(23), 5971-5980.

Andrade-Zapata, I., & Baonza, A. (2014). The bHLH factors extramacrochaetae and daughterless control cell cycle in Drosophila imaginal discs through the transcriptional regulation of the Cdc25 phosphatase string. *PLoS Genet, 10*(3), e1004233.

Aram, L., Yacobi-Sharon, K., & Arama, E. (2017). CDPs: caspase-dependent non-lethal cellular processes. *Cell Death Differ, 24*(8), 1307-1310.

Aza-Blanc, P., Ramirez-Weber, F. A., Laget, M. P., Schwartz, C., & Kornberg, T. B. (1997). Proteolysis that is inhibited by hedgehog targets Cubitus interruptus protein to the nucleus and converts it to a repressor. *Cell, 89*, 1043-1053.

Baena-Lopez, L. A., Arthurton, L., Xu, D. C., & Galasso, A. (2018). Non-apoptotic Caspase regulation of stem cell properties. *Semin Cell Dev Biol, 82*, 118-126.

Baker, N. E. (1988). Transcription of the segment-polarity gene wingless in the imaginal discs of Drosophila, and the phenotype of a pupal-lethal wg mutation. *Development, 102*(3), 489-497.

Baker, N. E., Bhattacharya, A., & Firth, L. C. (2009). Regulation of Hh signal transduction as Drosophila eye differentiation progresses. *Dev Biol, 335*(2), 356-366.

Baker, N. E., & Brown, N. L. (2018). All in the family: neuronal diversity and proneural bHLH genes. *Development, 145*, dev159426.

Baker, N. E., Li, K., Quiquand, M., Ruggiero, R., & Wang, L. H. (2014). Eye development. *Methods, 68*(1), 252-259.

Baker, N. E., Moses, K., Nakahara, D., Ellis, M. C., Carthew, R. W., & Rubin, G. M. (1992). Mutations on the second chromosome affecting the Drosophila eye. *J Neurogenet, 8*(2), 85-100.

Baker, N. E., & Yu, S. Y. (1998). The R8-photoreceptor equivalence group in *Drosophila* : fate choice precedes regulated *Delta* transcription and is independent of *Notch* gene dose. *Mechanisms of Development, 74*, 3-14.

Baonza, A., & Freeman, M. (2001a). Notch signalling and the initiation of neural development in the *Drosophila* eye. *Development, 128*, 3889-3898.

Baonza, A., & Freeman, M. (2001b). Notch signalling and the initiation of neural development in the Drosophila eye. *Development, 128*(20), 3889-3898.

Benezra, R., Davis, R. L., Lockshon, D., Turner, D. L., & Weintraub, H. (1990). The protein Id: a negative regulator of helix-loop-helix DNA binding proteins. *Cell, 61*(1), 49-59.

Bhattacharya, A., & Baker, N. E. (2009). The HLH protein Extramacrochaetae is required for R7 cell and cone cell fates in the Drosophila eye. *Dev Biol, 327*(2), 288-300.

Bhattacharya, A., & Baker, N. E. (2011). A network of broadly expressed HLH genes regulates tissue-specific cell fates. *Cell, 147*(4), 881-892.

Bhattacharya, A., & Baker, N. E. (2012). The Role of the bHLH Protein Hairy in Morphogenetic Furrow Progression in the Developing Drosophila Eye. *PLoS One, 7*(10), e47503.

Borod, E. R., & Heberlein, U. (1998). Mutual regulation of decapentaplegic and hedgehog during the initiation of differentiation in the Drosophila retina. *Dev Biol, 197*(2), 187-197.

Bray, S. J. (2006). Notch signalling: a simple pathway becomes complex. *Nat Rev Mol Cell Biol, 7*(9), 678-689.

Bray, S. J. (2016). Notch signalling in context. *Nat Rev Mol Cell Biol, 17*(11), 722-735.
Brown, N. L., Paddock, S. W., Sattler, C. A., Cronmiller, C., Thomas, B. J., & Carroll, S. B. (1996). *daughterless* is required for *Drosophila* photoreceptor cell determination, eye morphogenesis, and cell cycle progression. *Developmental Biology, 179*, 65-78.
Brown, N. L., Sattler, S. A., Paddock, S. W., & Carroll, S. B. (1995). *hairy* and *emc* negatively regulate morphogenetic furrow progression in the developing *Drosophila* eye. *Cell, 80*, 879-887.
Cabrera, C. V., Alonso, M. C., & Huikeshoven, H. (1994). Regulation of scute function by extramacrochaete in vitro and in vivo. *Development, 120*(12), 3595-3603.
Cadigan, K. M., Jou, A. D., & Nusse, R. (2002). Wingless blocks bristle formation and morphogenetic furrow progression in the eye through repression of Daughterless. *Development, 129*(14), 3393-3402.
Chang, J. L., Chang, M. V., Barolo, S., & Cadigan, K. M. (2008). Regulation of the feedback antagonist naked cuticle by Wingless signaling. *Dev Biol, 321*(2), 446-454.
Coelho, C. M., Kolevski, B., Bunn, C., Walker, C., Dahanukar, A., & Leevers, S. J. (2005). Growth and cell survival are unevenly impaired in pixie mutant wing discs. *Development, 132*(24), 5411-5424.
Colon-Plaza, S., & Su, T. T. (2022). Non-Apoptotic Role of Apoptotic Caspases in the Drosophila Nervous System. *Front Cell Dev Biol, 10*, 839358.
Cooper, M. T. D., & Bray, S. J. (2000). R7 photoreceptor specification requires N activity. *Current Biology, 10*, 1507-1510.
Daskalaki, A., Shalaby, N. A., Kux, K., Tsoumpekos, G., Tsibidis, G. D., Muskavitch, M. A., et al. (2011). Distinct intracellular motifs of Delta mediate its ubiquitylation and activation by Mindbomb1 and Neuralized. *J Cell Biol, 195*(6), 1017-1031.
Dennis, D. J., Han, S., & Schuurmans, C. (2019). bHLH transcription factors in neural development, disease, and reprogramming. *Brain Res, 1705*, 48-65.
Ellis, H. M. (1994). Embryonic expression and function of the Drosophila helix-loop-helix gene, extramacrochaetae. *Mech Dev, 47*(1), 65-72.
Ellis, H. M., Spann, D. R., & Posakony, J. W. (1990). extramacrochaetae, a negative regulator of sensory organ development in Drosophila, defines a new class of helix-loop-helix proteins. *Cell, 61*(1), 27-38.
Firth, L. C., Bhattacharya, A., & Baker, N. E. (2010). Cell cycle arrest by a gradient of Dpp signaling during Drosophila eye development. *BMC Dev Biol, 10*, 28.
Flores, G., Duan, H., Yan, H., Nagaraj, R., Fu, W., Zou, Y., et al. (2000). Combinatorial signaling in the specification of unique cell fates. *Cell, 103*, 75-85.
Fu, W., & Baker, N. E. (2003). Deciphering synergistic and redundant roles of Hedgehog, Decapentaplegic and Delta that drive the wave of differentiation in Drosophila eye development. *Development, 130*(21), 5229-5239.
Fuchs, Y., & Steller, H. (2011). Programmed cell death in animal development and disease. *Cell, 147*(4), 742-758.
Garcia-Alonso, L., & Garcia-Bellido, A. (1988). Extramacrochaetae a trans-acting gene of the Achaete-Scyte complex of *Drosophila* involved in cell communication. *Roux's Archives of Developmental Biology, 197*, 328-338.
Garrell, J., & Modolell, J. (1990). The Drosophila extramacrochaetae locus, an antagonist of proneural genes that, like these genes, encodes a helix-loop-helix protein. *Cell, 61*(1), 39-48.

Golic, K. G. (1991). Site-specific recombination between homologous chromosomes in Drosophila. *Science, 252*(5008), 958-961.

Hawkins, C. J., Yoo, S. J., Peterson, E. P., Wang, S. L., Vernooy, S. Y., & Hay, B. A. (2000). The Drosophila caspase DRONC cleaves following glutamate or aspartate and is regulated by DIAP1, HID, and GRIM. *J Biol Chem, 275*(35), 27084-27093.

Hawkins, C. J., Yoo, S. J., Peterson, E. P., Wang, S. L., Vernooy, S. Y., & Hay, B. A. (2000). The *Drosophila*caspase DRONC cleaves following glutamate or aspartate and is regulated by DIAP1, HID, and GRIM. *Journal of Biological Chemistry, 275*, 27084-27093.

Hay, B. A., Wolff, T., & Rubin, G. M. (1994). Expression of baculovirus P35 prevents cell death in *Drosophila*. *Development, 120*, 2121-2129.

Heberlein, U., Singh, C. M., Luk, A. Y., & Donohoe, T. J. (1995). Growth and differentiation in the *Drosophila* eye coordinated by *hedgehog*. *Nature, 373*, 709-711.

Heberlein, U., Wolff, T., & Rubin, G. M. (1993). The TGF beta homolog dpp and the segment polarity gene hedgehog are required for propagation of a morphogenetic wave in the Drosophila retina. *Cell, 75*(5), 913-926.

Heberlein, U., Wolff, T., & Rubin, G. M. (1993). The TGF-ß homolog *dpp* and the segment polarity gene *hedgehog* are required for propagation of a morphogenetic wave in the *Drosophila* retina. *Cell, 75*, 913-926.

Hepker, J., Wang, Q.-T., Motzny, C., Holmgren, R., & Orenic, T. V. (1997). *Drosophila cubitus interruptus* forms a negative feedback loop with *patched* and regulates expression of Hedgehog target genes. *Development, 124*, 549-558.

Ishibashi, T., Hatori, R., Maeda, R., Nakamura, M., Taguchi, T., Matsuyama, Y., et al. (2019). E and ID proteins regulate cell chirality and left-right asymmetric development in Drosophila. *Genes Cells, 24*(3), 214-230.

Jacobsen, T. L., Brennan, K., Martinez-Arias, A., & Muskavitch, M. A. (1998). Cis-interactions between Delta and Notch modulate neurogenic signalling in *Drosophila*. *Development, 125*, 4531-4540.

Jarman, A. P., Grell, E. H., Ackerman, L., Jan, L. Y., & Jan, Y. N. (1994). *atonal* is the proneural gene for *Drosophila* photoreceptors. *Nature, 369*, 398-400.

Jennings, B., Preiss, A., Delidakis, C., & Bray, S. (1994). The Notch signalling pathway is required for Enhancer of split bHLH protein expression during neurogenesis in the Drosophila embryo. *Development, 120*(12), 3537-3548.

Jimenez, F., & Campos-Ortega, J. A. (1987). Genes in subdivision 1B of the *Drosophila melanogaster* X-chromosome and their influence on neural development. *Journal of Neurogenetics, 4*, 179-200.

Johnson, J. E. (2020). bHLH factors in neurogenesis and neuronal subtype specification. In S. Temple & Q. Shen (Eds.), *Patterning and cell type specification in the developing CNS and PNS*: Academic Press.

Kale, A., Li, W., Lee, C. H., & Baker, N. E. (2015). Apoptotic mechanisms during competition of ribosomal protein mutant cells: roles of the initiator caspases Dronc and Dream/Strica. *Cell Death Differ, 22*(8), 1300-1312.

Kanuka, H., Kuranaga, E., Takemoto, K., Hiratou, T., Okano, H., & Miura, M. (2005). Drosophila caspase transduces Shaggy/GSK-3beta kinase activity in neural precursor development. *EMBO J, 24*(21), 3793-3806.

838 Kuranaga, E., & Miura, M. (2007). Nonapoptotic functions of caspases: caspases as regulatory
839 molecules for immunity and cell-fate determination. *Trends Cell Biol, 17*(3), 135-144.
840 Lee, J. D., & Treisman, J. E. (2002). Regulators of the morphogenetic furrow. *Results Probl Cell*
841 *Differ, 37*, 21-33.
842 Li, K., & Baker, N. E. (2018). Regulation of the Drosophila ID protein Extra macrochaetae by
843 proneural dimerization partners. *Elife, 7*, e33967.
844 Li, W., & Baker, N. E. (2007). Engulfment is required for cell competition. *Cell, 129*(6), 1215-
845 1225.
846 Li, X., Wang, J., & Shi, Y. (2011). Structural mechanisms of DIAP1 auto-inhibition and DIAP1-
847 mediated inhibition of drICE. *Nat Commun, 2*, 408.
848 Li, X. Y., MacArthur, S., Bourgon, R., Nix, D., Pollard, D. A., Iyer, V. N., et al. (2008).
849 Transcription factors bind thousands of active and inactive regions in the Drosophila
850 blastoderm. *PLoS Biol, 6*(2), e27.
851 Li, Y., & Baker, N. E. (2001). Proneural enhancement by Notch overcomes Suppressor-of-
852 Hairless repressor function in the developing *Drosophila* eye. *Current Biology, 11*, 330-
853 338.
854 Li, Y., & Baker, N. E. (2004). The roles of cis-inactivation by Notch ligands and of *neuralized*
855 during eye and bristle patterning in *Drosophila*. *BioMed Central Developmental Biology,*
856 *4*, 5.
857 Ling, F., Kang, B., & Sun, X. H. (2014). Id proteins: small molecules, mighty regulators. *Curr*
858 *Top Dev Biol, 110*, 189-216.
859 Little, J. C., Garcia-Garcia, E., Sul, A., & Kalderon, D. (2020). Drosophila hedgehog can act as a
860 morphogen in the absence of regulated Ci processing. *Elife, 9*.
861 Ma, C., & Moses, K. (1995). Wingless and patched are negative regulators of the morphogenetic
862 furrow and can affect tissue polarity in the developing Drosophila compound eye.
863 *Development, 121*, 2279-2289.
864 Ma, C., Zhou, Y., Beachy, P. A., & Moses, K. (1993). The segment polarity gene hedgehog is
865 required for progression of the morphogenetic furrow in the developing Drosophila eye.
866 *Cell, 75*(5), 927-938.
867 Massari, M. E., & Murre, C. (2000). Helix-loop-helix proteins: regulators of transcription in
868 eucaryotic organisms. *Mol Cell Biol, 20*(2), 429-440.
869 Maurel-Zaffran, C., & Treisman, J. E. (2000). pannier acts upstream of wingless to direct dorsal
870 eye disc development in Drosophila. *Development, 127*(5), 1007-1016.
871 Meier, P., Silke, J., Leevers, S. J., & Evan, G. I. (2000). The Drosophila caspase DRONC is
872 regulated by DIAP1. *EMBO J, 19*(4), 598-611.
873 Micchelli, C. A., Rulifson, E. J., & Blair, S. S. (1997). The function and regulation of cut
874 expression on the wing margin of Drosophila: Notch, Wingless and a dominant negative
875 role for Delta and Serrate. *Development, 124*, 1485-1495.
876 Miller, A. C., Lyons, E. L., & Herman, T. G. (2009). cis-Inhibition of Notch by endogenous
877 Delta biases the outcome of lateral inhibition. *Curr Biol, 19*(16), 1378-1383.
878 Motzny, C. K., & Holmgren, R. (1995). The *Drosophila* cubitus interruptus protein and its role
879 in the *wingless* and *hedgehog* signal transduction pathways. *Mechanisms of*
880 *Development, 52*, 137-150.
881 Muro, I., Hay, B. A., & Clem, R. J. (2002). The Drosophila DIAP1 protein is required to prevent
882 accumulation of a continuously generated, processed form of the apical caspase DRONC.
883 *J Biol Chem, 277*(51), 49644-49650.

884 Nakajima, Y. I., & Kuranaga, E. (2017). Caspase-dependent non-apoptotic processes in
885 development. *Cell Death Differ, 24*(8), 1422-1430.
886 Norton, J. D. (2000). ID helix-loop-helix proteins in cell growth, differentiation and
887 tumorigenesis. *J Cell Sci, 113 (Pt 22)*, 3897-3905.
888 Ohlmeyer, J. T., & Kalderon, D. (1998). Hedgehog stimulates maturation of Cubitus interruptus
889 into a labile transcriptional activator. *Nature, 396*(6713), 749-753.
890 Oproescu, A. M., Han, S., & Schuurmans, C. (2021). New Insights Into the Intricacies of
891 Proneural Gene Regulation in the Embryonic and Adult Cerebral Cortex. *Front Mol*
892 *Neurosci, 14*, 642016.
893 Ou, C. Y., Lin, Y. F., Chen, D. F., & Chien, C. T. (2002). Distinct protein degradation
894 mechanisms mediated by Cul1 and Cul3 controlling Ci stability in *Drosophila* eye
895 development. *Genes and Development, 16*, 2403-2414.
896 Parks, A. L., Turner, R. F., & Muskavitch, M. A. T. (1995). Relationships between complex
897 Delta expression and the specification of retinal fates during *Drosophila* eye
898 development. *Mechanisms of Development, 50*, 201-216.
899 Pignoni, F., & Zipursky, L. (1997). Induction of *Drosophila* eye development by
900 Decapentaplegic. *Development, 124*, 271-278.
901 Quinn, L. M., Dorstyn, L., Mills, K., Colussi, P. A., Chen, P., Coombe, M., et al. (2000). An
902 essential role for the caspase dronc in developmentally programmed cell death in
903 Drosophila. *J Biol Chem, 275*(51), 40416-40424.
904 Reddy, V., Bhattacharya, A., & Baker, N. E. The Id protein Extramacrochaetae restrains the E-
905 protein Daughterless to regulate Notch, Rap1, and Sevenless within the R7 equivalence
906 group of the Drosophila eye *Biology Open, submitted*.
907 Roschger, C., & Cabrele, C. (2017). The Id-protein family in developmental and cancer-
908 associated pathways. *Cell Commun Signal, 15*(1), 7.
909 Sato, A., Kojima, T., Ui-Tei, K., Miyata, Y., & Saigo, K. (1999). Dfrizzled-3, a new Drosophila
910 Wnt receptor, acting as an attenuator of Wingless signaling in wingless hypomorphic
911 mutants. *Development, 126*(20), 4421-4430.
912 Shi, W., Stampas, A., Zapata, C., & Baker, N. E. (2003). The pineapple eye gene is required for
913 survival of Drosophila imaginal disc cells. *Genetics, 165*(4), 1869-1879.
914 Singh, S., Sarkar, T., Jakubison, B., Gadomski, S., Spradlin, A., Gudmundsson, K. O., et al.
915 (2022). Inhibitor of DNA binding proteins revealed as orchestrators of steady state, stress
916 and malignant hematopoiesis. *Front Immunol, 13*, 934624.
917 Spratford, C. M., & Kumar, J. P. (2013). Extramacrochaetae imposes order on the Drosophila
918 eye by refining the activity of the Hedgehog signaling gradient. *Development, 140*(9),
919 1994-2004.
920 Struhl, G., & Greenwald, I. (1999). Presenilin is required for activity and nuclear access of Notch
921 in Drosophila. *Nature, 398*(6727), 522-525.
922 Su, T. T. (2020). Non-apoptotic roles of apoptotic proteases: new tricks for an old dog. *Open*
923 *Biol, 10*(8), 200130.
924 Tapadia, M. G., & Gautam, N. K. (2011). Non-apoptotic function of apoptotic proteins in the
925 development of Malpighian tubules of Drosophila melanogaster. *J Biosci, 36*(3), 531-
926 544.
927 Tomlinson, A., & Struhl, G. (2001). Delta/Notch and Boss/Sevenless signals act combinatorially
928 to specify the *Drosophila* R7 photoreceptor. *Molecular Cell, 7*, 487-495.

929 Treisman, J. E. (2013). Retinal differentiation in Drosophila. *Wiley Interdiscip Rev Dev Biol,*
930 *2*(4), 545-557.
931 Treisman, J. E., & Rubin, G. M. (1995). wingless inhibits morphogenetic furrow movement in
932 the Drosophila eye disc. *Development, 121*(11), 3519-3527.
933 Verghese, S., Bedi, S., & Kango-Singh, M. (2012). Hippo signalling controls Dronc activity to
934 regulate organ size in Drosophila. *Cell Death Differ, 19*(10), 1664-1676.
935 Vrailas, A. D., & Moses, K. (2006). Smoothened, thickveins and the genetic control of cell cycle
936 and cell fate in the developing Drosophila eye. *Mech Dev, 123*(2), 151-165.
937 Wang, L. H., & Baker, N. E. (2015a). E Proteins and ID Proteins: Helix-Loop-Helix Partners in
938 Development and Disease. *Dev Cell, 35*(3), 269-280.
939 Wang, L. H., & Baker, N. E. (2015b). Salvador-Warts-Hippo pathway in a developmental
940 checkpoint monitoring helix-loop-helix proteins. *Dev Cell, 32*(2), 191-202.
941 Wang, L. H., & Baker, N. E. (2018). Spatial regulation of expanded transcription in the
942 Drosophila wing imaginal disc. *PLoS One, 13*(7), e0201317.
943 Wang, L. H., & Baker, N. E. (2019). Salvador-Warts-Hippo pathway regulates sensory organ
944 development via caspase-dependent nonapoptotic signaling. *Cell Death Dis, 10*(9), 669.
945 Wang, M., Zhao, X. M., Tan, H., Akutsu, T., Whisstock, J. C., & Song, J. (2014). Cascleave 2.0,
946 a new approach for predicting caspase and granzyme cleavage targets. *Bioinformatics,*
947 *30*(1), 71-80.
948 Weinberger, S., Topping, M. P., Yan, J., Claeys, A., De Geest, N., Ozbay, D., et al. (2017).
949 Evolutionary changes in transcription factor coding sequence quantitatively alter sensory
950 organ development and function. *Elife, 6*.
951 White, K., Grether, M. E., Abrams, J. M., Young, L., Farrell, K., & Steller, H. (1994). Genetic
952 control of programmed cell death in Drosophila. *Science, 264*(5159), 677-683.
953 Wilson, R., Goyal, L., Ditzel, M., Zachariou, A., Baker, D. A., Agapite, J., et al. (2002). The
954 DIAP1 RING finger mediates ubiquitination of Dronc and is indispensable for regulating
955 apoptosis. *Nat Cell Biol, 4*(6), 445-450.
956 Xu, T., & Rubin, G. M. (1993). Analysis of genetic mosaics in developing and adult Drosophila
957 tissues. *Development, 117*(4), 1223-1237.
958 Xue, D., & Horvitz, H. R. (1995). Inhibition of the *Caenorhabditis elegans* cell-death protease
959 CED-3 by a CED-3 cleavage site in baculovirus p35 protein. *Nature, 377*, 248-251.
960 Yamaguchi, Y., & Miura, M. (2015). Programmed Cell Death and Caspase Functions During
961 Neural Development. *Curr Top Dev Biol, 114*, 159-184.
962 Yan, N., Wu, J. W., Chai, J., Li, W., & Shi, Y. (2004). Molecular mechanisms of DrICE
963 inhibition by DIAP1 and removal of inhibition by Reaper, Hid and Grim. *Nat Struct Mol*
964 *Biol, 11*(5), 420-428.
965 Ye, Y., Lukinova, N., & Fortini, M. E. (1999). Neurogenic phenotypes and altered Notch
966 processing in Drosophila Presenilin mutants. *Nature, 398*(6727), 525-529.
967 Yoo, S. J., Huh, J. R., Muro, I., Yu, H., Wang, L., Wang, S. L., et al. (2002). Hid, Rpr, and Grim
968 negatively regulate DIAP1 levels through distinct mechanisms. *Nature Cell Biology, 4*,
969 416-424.
970 Zeng, W., Wharton, K. A., Mack, J. A., Wang, K., Gadbaw, M., Suyama, K., et al. (2000). *naked*
971 *cuticle* encodes an inducible antagonist of Wnt signalling. *Nature, 403*, 789-795.
972